



THE HONG KONG
POLYTECHNIC UNIVERSITY

香港理工大學

Pao Yue-kong Library
包玉剛圖書館

Copyright Undertaking

This thesis is protected by copyright, with all rights reserved.

By reading and using the thesis, the reader understands and agrees to the following terms:

1. The reader will abide by the rules and legal ordinances governing copyright regarding the use of the thesis.
2. The reader will use the thesis for the purpose of research or private study only and not for distribution or further reproduction or any other purpose.
3. The reader agrees to indemnify and hold the University harmless from and against any loss, damage, cost, liability or expenses arising from copyright infringement or unauthorized usage.

If you have reasons to believe that any materials in this thesis are deemed not suitable to be distributed in this form, or a copyright owner having difficulty with the material being included in our database, please contact lbsys@polyu.edu.hk providing details. The Library will look into your claim and consider taking remedial action upon receipt of the written requests.

**Effect of Acoustic Pressure Waves on Callus Innervation
and Fracture Healing**

Wai Ling Lam

**A thesis submitted in partial fulfilment of the requirements for the
Degree of Master of Philosophy**

Department of Rehabilitation Sciences

The Hong Kong Polytechnic University

June 2005

Certificate of Originality

I hereby declare that this thesis is my own work and that, to the best of my knowledge and belief, it reproduces no material previously published or written nor material which has been accepted for the award of any other degree or diploma, except where due acknowledgement has been made in the text.

_____ (Signed)

LAM WAI LING (Name of student)

Table of Contents

Acknowledgements	i
List of Tables	iii
List of Figures	iv
Abstract	vii
Chapter 1 Introduction	1
Chapter 2 Literature review	2
2.1 Normal structure and function of bone	2
2.1.1 Functions of bone	2
2.1.2 The matrix of bone	2
2.1.3 Types and functions of bone cells	3
2.1.4 Structures of bone	5
2.1.5 The periosteum and endosteum	8
2.1.6 Bone development and growth	8
2.2 Fracture healing	10
2.2.1 Mechanisms of fracture healing	11
2.2.2 Fracture healing in rats	13
2.3 Low intensity pulsed ultrasound and fracture healing	14
2.3.1 Types and functions of ultrasound	14
2.3.2 Physiological effects of ultrasound	15
2.3.3 Evidences of LIPU accelerating fracture healing	15

2.3.4	Effect of LIPU on different stages of fracture healing	17
	Effect of LIPU on inflammatory phase	17
	Effect of LIPU on reparative phase	18
	Effect of LIPU on chondrogenesis	18
	Effect of LIPU on osteogenesis	19
	Effect of LIPU on blood flow and neovascularization	19
	Effect of LIPU on remodeling phase	19
2.3.5	Efficacious signal parameters of LIPU	20
2.4	Bone innervation and fracture healing	21
Chapter 3	Objectives and significance of the study	23
Chapter 4	Methodology	25
4.1	Animal Model	25
4.2	Ethical considerations	25
4.3	Study Design	25
4.4	Surgical Procedures	28
4.4.1	Tibial fracture model	28
4.4.2	Resection of sciatic nerve	30
4.4.3	Resection of the patella tendon	31
4.4.4	LIPU treatment	32
4.5	Outcome evaluation	33
4.5.1	Radiographic evaluation	33
4.5.2	Bone densitometry	34
4.5.3	Mechanical testing	36

4.5.4	Histomorphometry	39
4.6	Statistical analysis	41
Chapter 5	Results	42
5.1	Radiographic evaluation	42
5.1.1	Callus index	42
5.1.2	Union rate	43
5.2	Densitometry by pQCT	45
5.2.1	Total BMD	45
5.2.2	Total BMC	48
5.2.3	Total BA	49
5.3	Mechanical Testing	50
5.3.1	Ultimate load from four-point bending test	50
5.3.2	Stiffness from four-point bending test	52
5.3.3	Union rate assessed during pin removal	53
5.4	Correlations	54
5.4.1	Correlations between callus size evaluated by radiograph and pQCT	54
5.4.2	Correlations between bone strength-related parameters obtained from pQCT and those from four-point bending test	54
5.5	Histomorphometry	55
Chapter 6	Discussion	63
6.1	Effectiveness of LIPU in enhancing fracture healing	63

6.2	Role of innervation in response to LIPU on fracture healing	64
6.3	Influence of nerve resection on fracture healing	65
6.4	Bone mineral content	66
6.5	Ultimate load and stiffness from four-point bending test	67
6.6	Mechanical test findings from previous studies on LIPU	70
6.7	Mechanical test findings from previous studies on nerve resection	71
6.8	Correlations on bone strength	71
6.9	Correlations on callus size	73
6.10	Histological findings	74
6.11	Limitations	74
Chapter 7	Conclusions	76
	References	77
	Appendix I	85
	Appendix II	86
	Appendix III	88
	Conference abstracts	

Acknowledgements

First of all, I would like to express my gratitude to my chief supervisor, Dr. Xia Guo, for her guidance, encouragement and continual support throughout my studies. The work described in this dissertation depended upon her initial inspiration and continuing assistance.

I would also like to deeply thank my co-supervisor Dr. Kevin Kwong, and Prof. K.S. Leung (from the Department of Orthopaedics and Traumatology, The Chinese University of Hong Kong), for their valuable advice and support.

I am also grateful Dr. Ella Yeung for her helpful comments and suggestions with regard to this study.

Mr. Peggo Lam is highly praised for his extensive assistance in statistical analysis.

I would also like to thank Dr. Ming Zhang, Mr. Jason Cheung and Miss Anita Shum from the Department of Rehabilitation Engineering Centre, The Hong Kong Polytechnic University, for kindly arranging laboratory facilities and technical support for the mechanical tests carried out in this study.

Thanks are further extended to my colleagues, Mr. Benny Hui, Dr. Mu Qing Liu, Miss Xiao Yun Wong, Mr. Chi Keung Yeung, Mr. Ka Keung Yip, and Dr. Yong Fang Zhao, for their help, support and encouragement throughout my studies.

Sincere appreciation is expressed to my colleagues, Dr. Francis Chan, Dr. Louis Cheung, Miss Cathie Fok, Miss Vivien Hung, Miss Winnie Lee, Mr. Sammy Siu and Mr. Benson Yeung from the Department of Orthopaedic and Traumatology, The Chinese University of Hong Kong, for their support and encouragement during the past two years.

I must also thank the staff working in the Centralized Animal Facilities in the Hong Kong Polytechnic University, for taking good care of the animals used in this study.

The sacrifice of the animals used in this study is highly appreciated for allowing us to extend our knowledge and understanding of the effects of Low Intensity Pulsed Ultrasound (LIPU) and neural influence, as well as the relationship between these two factors on fracture healing.

The encouragement and spiritual support from my family members and my boyfriend, Mr. Rex Chu, are also much appreciated.

Last but not least, I would like to acknowledge the Hong Kong Research Grant Committee for providing financial support for this study (RGC Grant PolyU 5273/02M).

List of Tables

Table 1	Treatments on different groups	27
Table 2	Evaluation Methods	27
Table 3	Distribution of animals for radiographic evaluation in different groups	43
Table 4	Results of intra-class correlation coefficients (ICC) between the two assessors	43
Table 5	Results of callus index in each treatment group	43
Table 6	Results obtained from pQCT measurements in each treatment group	46
Table 7	Results of Bonferroni's multiple comparison test for total BMD	46
Table 8	Results on ultimate load and stiffness obtained from four-point bending test in each treatment group	50
Table 9	Correlations between bone strength-related parameters obtained from pQCT and those from four-point bending test	54

Lists of Figures

Figure 1	Histomorphology of compact bone	3
Figure 2	Different types of bone cells at the site of remodeling	5
Figure 3	Structure of osseous tissue	7
Figure 4	Typical waveform of pulsed ultrasound	14
Figure 5	A device for creating fracture	28
Figure 6	Fracture creating method	28
Figure 7	Lateral tibial radiograph for evaluating the position and orientation of the fracture	29
Figure 8	Surgical resection of sciatic nerve	30
Figure 9	Surgical resection of patella tendon	31
Figure 10	Specifications of ultrasound machine (SAFHS, Exogen Inc, NJ, USA)	32
Figure 11	pQCT machine (XCT 2000, Norland Stratec, Germany)	35
Figure 12	Position of each slice for scanning	35
Figure 13	Data retrieval by the machine	35
Figure 14	Hounsfield Material Testing Machine (H10KM, Hounsfield Test Equipment, UK) with a 1000N load cell	37
Figure 15	Set up and orientation of the specimen for four-point bending test	38

Figure 16	Load-displacement curve generated by the computer system of the mechanical testing machine	38
Figure 17	Tissue Processor (Shadon, England)	40
Figure 18	Results of two-way ANOVA for callus index	44
Figure 19	Results on union rate evaluated from x ray in each treatment group	44
Figure 20	Results of two-way ANOVA for total BMD assessed by pQCT	47
Figure 21	Results of two-way ANOVA for total BMC assessed by pQCT	48
Figure 22	Results of two-way ANOVA for total BA assessed by pQCT	49
Figure 23	Results of two-way ANOVA for ultimate load	51
Figure 24	Results of two-way ANOVA for stiffness	52
Figure 25	Results on union rate obtained during pin removal before four-point bending test in each treatment group	53
Figure 26	Sham LIPU neural intact group at 7 days post-fracture (H&E, 100x)	57
Figure 27	LIPU neural intact group at 7 days post-fracture (H&E, 100x)	57

Figure 28	Sham LIPU neurectomy group at 7 days post-fracture (H&E, 100x)	58
Figure 29	LIPU neurectomy group at 7 days post-fracture (H&E, 100x)	58
Figure 30	Sham LIPU neural intact group at 14 days post-fracture (H&E, 100x)	59
Figure 31	LIPU neural intact group at 14 days post-fracture (H&E, 100x)	59
Figure 32	Sham LIPU neurectomy group at 14 days post-fracture (H&E, 100x)	60
Figure 33	LIPU neurectomy group at 14 days post-fracture (H&E, 100x)	60
Figure 34	Sham LIPU neural intact group at 21 days post-fracture (H&E, 100x)	61
Figure 35	LIPU neural intact group at 21 days post-fracture (H&E, 100x)	61
Figure 36	Sham LIPU neurectomy group at 21 days post-fracture (H&E, 100x)	62
Figure 37	LIPU neurectomy group at 21 days post-fracture (H&E, 100x)	62

Abstract

Fracture healing is a highly complex regenerative process which includes the action of many different cell types. Low Intensity Pulsed Ultrasound (LIPU) has been shown an effective modality for enhancing fracture healing but the mechanism of which is still not well understood. Innervation in bone has been found to play an important role in fracture healing. It has been demonstrated that sensory nerve fibers were found to be reduced or absent in nonunions. LIPU transfers mechanical energy into tissues. This study was to test the hypothesis that sensory nerves in bone may play a role in sensing and responding to the mechanical stimulation provided by LIPU, and in turn, promotes fracture healing.

A diaphyseal transverse fracture was created on the right tibia in 120 matured female Sprague-Dawley rats (weight 261.44 ± 18.38 g, at 12 weeks of age) in this study. They were assigned randomly into 4 groups: the sham LIPU neural intact group, the LIPU neural intact group, the sham LIPU neurectomy group and the LIPU neurectomy group. For animals in the LIPU treated groups, LIPU was given daily at the fracture site starting on the 2nd day after the fracture was created. Sham exposure was introduced to those animals in the sham LIPU treated groups. Resection of the sciatic nerve of the fractured limb was performed on the animals in the neurectomy groups. In order to facilitate similar immobilization as that caused by sciatic neurectomy, patella tenotomy was employed on animals in the neural intact groups. Rats were sacrificed for tissue morphometrical analyses and

biomechanical testing on days 7, 14 and 21 post-fracture, according to the groups to which they belonged. Two-way ANOVA was used for statistical comparisons among the four groups ($\alpha=0.05$).

Results on the callus index evaluated from X-rays demonstrated that there was a significant main effect of innervation ($p<0.01$) on callus size where larger callus was found in the groups with neurectomy. Results on union rates obtained from X-rays and those obtained during pin removal before mechanical testing (palpation) showed a higher union rate in the two neural intact groups, with the highest union rate in the LIPU treated neural intact group (73% from X-ray and 89% from palpation before mechanical testing). Meanwhile, the union rate was comparable between the two groups with nerve resection. Results on total bone mineral density (BMD) indicated a significant interaction ($p<0.05$) between the two factors (innervation and LIPU). Results on the Bonferroni multiple comparison test suggested that the introduction of LIPU could significantly increase the total BMD in the fractured callus ($p<0.05$) in the neural intact limbs. However, such an increase in total BMD, caused by the introduction of LIPU, was not found in the limbs with sciatic neurectomy. Results on morphological studies indicated that groups with intact nerves healed better and faster than those without, and that a more matured callus was found in the LIPU-treated group when compared with the sham treated group in the groups with intact nerves. The rate of maturation was similar in the two groups with nerve resection.

The results of the present study confirm the accelerating effect of LIPU on fracture healing. Denervation could delay the healing of a fracture by developing a larger yet immature callus (as observed from results on union rate and morphological studies). The results also demonstrated that with the resection of sciatic nerve, the promoting effect of LIPU on fracture healing could greatly be reduced. This implies the importance of the callus innervation in sensing and responding to the mechanical stimulus generated by LIPU on fracture healing.

Chapter 1 Introduction

Repair of fractures involves a sequence of dynamic events which ultimately restore the integrity of the bone and its biomechanical properties. Low Intensity Pulsed Ultrasound (LIPU) is an effective modality used frequently in enhancing fracture healing (Hajiargyrou et al, 1998, Leung et al, 2004, Nolte et al, 2001). However, the mechanism of which is still not well understood. Recently, it has been found that innervation in bone play an important role in fracture healing (Hukkanen et al, 1993, Konttinen et al, 1996, Madsen et al, 2000, Norsletten et al, 1994, Onuoha, 2001, Onuoha & Alpar, 2000). It has been demonstrated that sensory nerve fibers were found to be reduced or absent in delayed union or nonunions (Aro, 2001, Dyck et al, 1983, Zaidi, 1988). LIPU transfers mechanical energy into tissues, thus it is important to relate the mechanical basis of ultrasound to the sensitivity of bone tissue through its sensory nerve fibers to mechanical stimuli. Up to now, there was no report addressing this relationship. The aim of this study was to investigate the role of bone innervation in response to LIPU for enhancing fracture healing.

Injuries to the peripheral or central nervous system are common complications associated with fractures. LIPU is an effective physiotherapy modality for enhancing fracture healing generally, but its effect on the healing of fractures accompanied with neural complications has not been explored. Outcome of this study will update our current understanding and expand our knowledge on the relationship between callus innervation and LIPU on fracture healing.

Chapter 2 Literature Review

2.1 Normal structure and function of bone

2.1.1. Functions of bone

Bone tissue is an essential component of the body that serves many purposes. It provides a framework for the attachment of muscles, tendons and ligaments, and facilitates kinematics motion. Bone also supports and provides protection to the soft tissues and vital internal organs (Remedios, 1999). It not only serves as storage for inorganic matrixes such as calcium and phosphorus and releases these substances on demand, but also participates in blood cell production (Martini, 2004).

2.1.2. The matrix of bone

Bone comprises 70% inorganic salts and 30% organic matrix by weight. The mineral component of bone mainly consists of calcium and phosphate in the form of hydroxyapatite crystals, $\text{Ca}_{10}(\text{PO}_4)_6(\text{OH})_2$. Collagen, almost exclusively in the form of type I fibers, makes up over 90% of the organic component. Collagen fibers provide an organic framework on which hydroxyapatite crystals can form. These crystals form small plates and rods that are locked and deposited into the collagen fibers. The remaining organic components are ground substance proteoglycans and a group of noncollagen molecules which appear to be involved in the regulation of bone mineralization. Cells account for only two percent of the mass of a typical bone (Konttinen et al, 1996, Young & Heath, 2000).

2.1.3. Types and functions of bone cells

There are four different cell types found in bone, namely, osteocytes, osteoblasts, bone-lining cells and osteoclasts. They are responsible for bone formation and remodeling (Martini, 2004).

Osteocytes (Figure 1) are mature bone cells that account for most of the cell population. They are inactive osteoblasts trapped within formed bone. The main function of osteocytes is to maintain and monitor the protein and mineral content of the surrounding bone matrix.

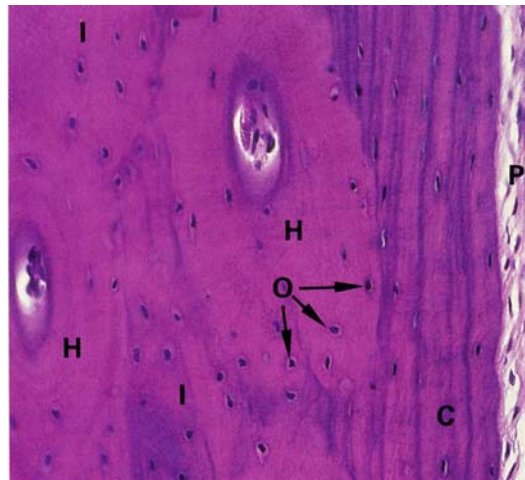


Figure 1 Histomorphology of compact bone.
C – Cortical bone, **H** – Haversian system, **I** – Interstitial lamellae,
O – Osteocytes, **P** – Periosteum. (from Young & Heath, 2000)

Osteoblasts (Figures 2a & b) are found lined up along the bone surface. They produce new bone matrix through a process called osteogenesis, in which they synthesize osteoid (unmineralized bone matrix) and mediate its mineralization. Osteocytes and osteoblasts are derived from a primitive mesenchymal cell called osteoprogenitor cells.

Bone-lining cells are located in the inner, cellular layer of the periosteum, in an inner layer, or endosteum, that lines marrow cavities, and in the lining of vascular passageways in the matrix. Bone-lining cells maintain populations of osteoblasts and are important in the repair of a fracture.

Osteoclasts (Figures 2a & c) are giant (20-100nm in diameter) multinucleated cells (with 50 or more nuclei). They are phagocytic cells derived from the macrophage-monocyte cell line. They are located at or near the surface of the bone and are capable of eroding bone by a process called osteolysis, in which they dissolve the matrix and release the stored minerals by secreting acid and proteolytic enzymes. They are important, together with osteoblasts, in regulating the constant rate of bone formation and resorption (Martini, 2004, Remedios, 1999, Young & Heath, 2000).

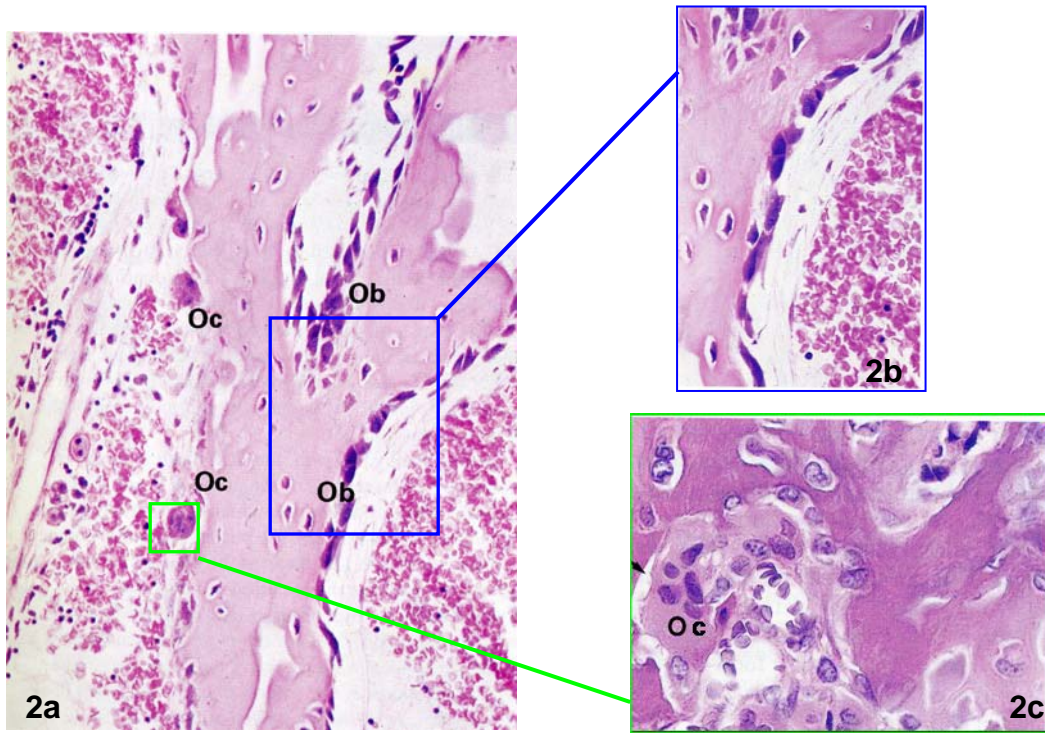


Figure 2 Different types of bone cells at the site of remodeling.
Ob – Osteoblast, **Oc** – Osteoclast (from Young & Heath, 2000)

2.1.4. Structures of bone

In the individual bone, two types of bone tissue are distinguishable, namely, compact bone and spongy bone (Figure 3). Compact bone is always located on the surface of a bone, where it forms a sturdy protective layer, while spongy bone makes up the interior of a bone (Martini, 2004).

The basic functional unit of mature compact bone is osteon, or the Haversian system. In an osteon, the osteocytes are arranged in concentric layers of lamella around a central canal, or Haversian canal, which contains blood vessels, lymphatics and nerves. Other passageways, known as perforating canals, or the canals of Volkmann, extend roughly perpendicular to the Haversian canal. Blood vessels in these canals supply blood to osteons deeper in the bone, and to the tissues of the marrow cavity. Within each lamella are the lacunae that house individual osteocytes. Between adjacent lacunae and the central canal are numerous minute interconnecting canals known as canaliculi, which contain fine cytoplasmic extensions of the osteocytes. Canaliculi allow exchanges of nutrients and waste products in osteocytes (Greenbaum & Kanat, 1993, Martini, 2004, Remedios, 1999, Young & Heath, 2000). During the growth of bone, continuous resorption and redeposition of bone take place, and interstitial lamellae and circumferential lamellae are formed. Interstitial lamellae bridge the spaces between the osteons. Circumferential lamellae are found at the outer and inner surfaces of the bone, where they are covered by the periosteum and endosteum, respectively (Martini, 2004, Remedios, 1999).

In spongy bone, lamellae are not arranged in osteons. The matrix in spongy bone forms struts and plates known as trabeculae. No capillaries or venules can be found in the matrix of spongy bone. Red marrow is found between the trabeculae of spongy bone, and blood vessels within this tissue provide nourishment to the osteocytes (Greenbaum & Kanat, 1993, Martini, 2004).

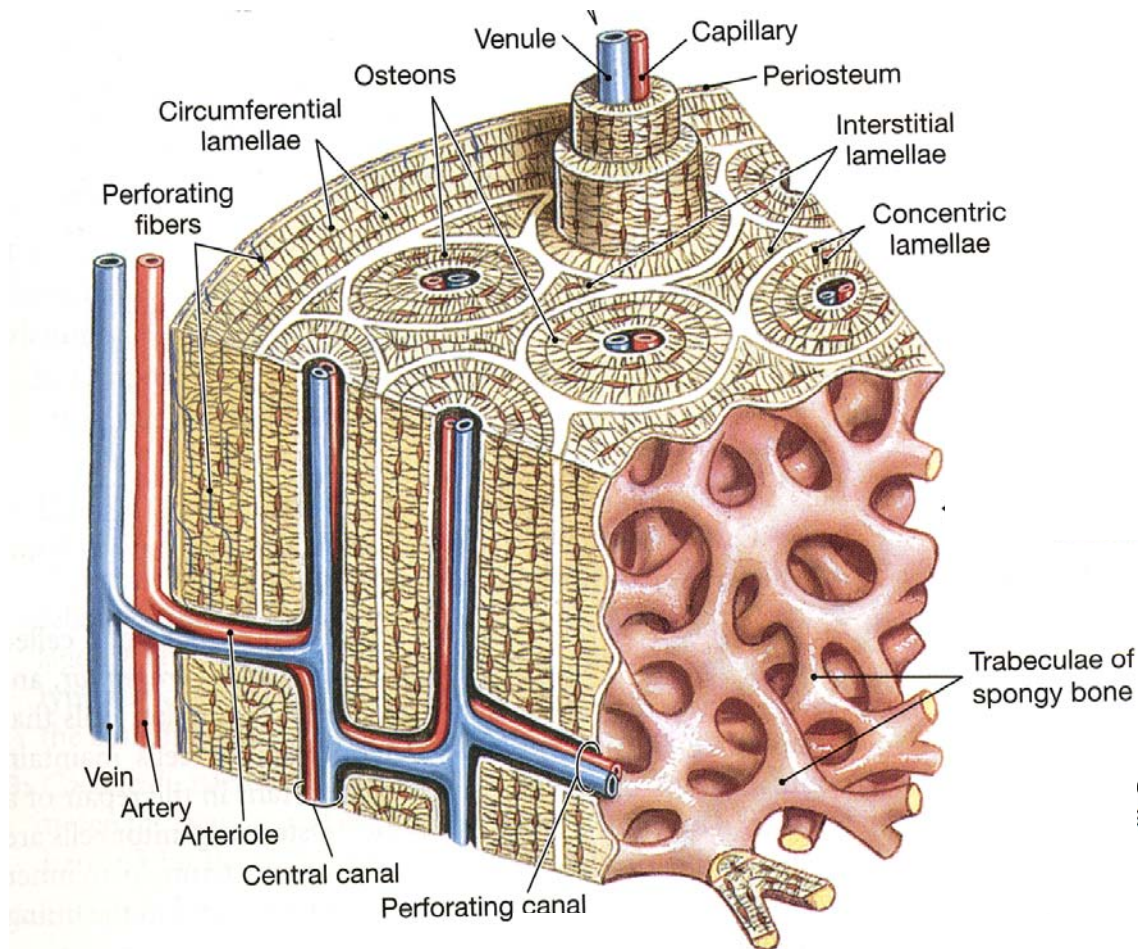


Figure 3 Structure of osseous tissue. (from Martini, 2004)

2.1.5. The periosteum and endosteum

Except within joint cavities, the outer surface of compact bone is covered by a membrane with a fibrous outer layer and a cellular inner layer, known as the periosteum (Martini, 2004, Young & Heath, 2000). The periosteum serves three functions: 1. it isolates bone from the surrounding tissues; 2. it provides a route for the circulatory and nervous supply, and 3. it actively participates in bone growth and repair (Martini, 2004).

The endosteum is an incomplete cellular layer of osteoprogenitor cells that lines the marrow cavity. The endosteum is active during bone growth, repair and remodeling (Martini, 2004).

2.1.6. Bone development and growth

Ossification is a term describing the formation of bone by replacing other tissues with bone. There are two types of ossification, intramembranous ossification and endochondral ossification (Martini, 2004, Young & Heath, 2000).

Intramembranous ossification involves direct replacement of the mesenchyme or fibrous connective tissue by bone. Briefly, it begins when osteoblasts differentiate within a mesenchymal or fibrous connective tissue. An osteoid is then synthesized and secreted by the osteoblasts at multiple centers of ossification. Followed by mineralization of the osteoid, some of the osteoblasts are trapped in the lacunae and become osteocytes. Progressive bone formation results in the fusion of adjacent

ossification centers to form spongy bone. Blood vessels then begin to grow into the area to supply nutrients to the region. After subsequent remodeling, structures typical to compact bone are formed (Martini, 2004, Young & Heath, 2000).

In endochondral ossification, bone replaces existing cartilage. Briefly, chondrocytes within the shaft of the cartilage begin to be enlarged greatly in size. The cartilage matrix is reduced to a series of thin struts and soon begins to calcify. The chondrocytes are then degenerated, leaving large, interconnecting spaces. Blood vessels start to grow into the perichondrium surrounding the shaft of the cartilage. The perichondrium then develops osteogenic potential and acts as periosteum. Blood vessels, together with fibroblasts, penetrate the cartilage and invade the central region. Fibroblasts are then differentiated into osteoblasts and begin to produce spongy bone at a primary center of ossification. Osteoclasts appear as the bone enlarges, initiate remodeling and create a marrow cavity. A secondary ossification center is created upon the migration of capillaries and osteoblasts into the epiphyses, which are then filled with spongy bone. Articular cartilage, a thin layer of the original cartilage model, remains exposed to the joint cavity. At each metaphysis, the epiphyseal cartilage, a relatively narrow cartilaginous region, separates the epiphysis from the diaphysis (Martini, 2004, Young & Heath, 2000).

2.2 Fracture healing

A fracture occurs whenever the upper limit of bone strain is exceeded (Simmons, 1985). It is estimated that there are 5.6 million fractures that occur annually in the United States, 5 to 10% of which demonstrate delayed union or nonunion (Einhorn, 1995). According to the American Academy of Orthopaedic Surgeons (2002), it is estimated that each person, on average, experiences two bone fractures over the course of a lifetime. According to the National Osteoporosis Foundation (2003), only 15% of hip fracture patients can walk across a room unaided 6 months after a fracture. An estimated 24% of hip fracture patients older than 50 years of age die within one year of their fracture. The high incidence of fractures, either union or non union, results in high economic expenditure on fracture treatments. Together with the immobility and morbidity it might introduce to patients, this makes it necessary for researchers to investigate the causes, factors involved, and ways to enhance the healing of a fracture.

2.2.1. Mechanisms of fracture healing

Fracture healing is a highly complex regenerative process which includes the action of many different cell types, genes expression and finally, the restoration of the natural integrity of the bone (Hadjiargyrou et al, 1998, Simmons, 1985). Three predominant stages are involved in fracture healing, namely, the inflammatory, reparative and remodeling phases. These phases are interrelated and overlap temporally (Hadjiargyrou et al, 1998, LaStayo et al, 2003, Martini, 2004, Remedios, 1999).

In the inflammatory phase, hematoma is formed as a result of blood vessels ruptured by the injury. Inflammatory cells, including lymphocytes, macrophages and mast cells, invade the clot and initiate the lysosomal degradation of necrotic tissue (Adams, 1999, Einhorn, 1998, Hadjiargyrou et al, 1998, LaStayo et al, 2003).

The reparative phase is characterized by the formation of a callus. It begins with the invasion of pluripotential mesenchymal stem cells, which differentiate into fibroblasts, chondroblasts, and osteoblasts (Hadjiargyrou et al, 1998, LaStayo et al, 2003, Martini, 2004). Osteoblasts directly deposit bone at farther site of the fracture by intramembranous ossification. Chondroblasts form cartilage adjacent to the fracture site, which is gradually replaced with new bone by endochondral ossification (Augat & Ryaby, 2001, Einhorn, 1998). Blood vessels are formed at this stage within the periosteal tissues and marrow space as a result of angiogenesis (Hadjiargyrou et al, 1998, Remedios, 1999).

The remodeling phase is the final phase of the healing process. It is characterized by the slow modeling and remodeling of the fracture callus from woven to mature lamellar bone, and ultimately, the restoration of the bone to normal or near normal morphology and mechanical strength (Greenbaum & Kanat, 1993, Hadjiargyrou et al, 1998, Martini, 2004, Remedios, 1999).

Many growth factors and regulatory proteins, such as platelets-derived growth factor (PDGF), transforming growth factor beta (TGF- β), bone morphogenetic protein (BMP), insulin-like growth factors I and II (IGF-I & II) as well as fibroblast growth factor (FGF), have been found to be synthesized by various tissue and cell types during fracture healing. In both *in vitro* and *in vivo* studies, these factors have been demonstrated to have different effects on cell proliferation, differentiation, and matrix production as related to bone repair (Cornell & Lane, 1992, Lind, 1996, Simmons, 1985).

2.2.2 Fracture healing in rats

In rats, fractures of long bone completely united at 35 days after fracture (Einhorn, 1998, Madsen et al, 1998). Similar to human, the three healing stages mentioned are involved in fracture healing in rats. Approximately, the inflammatory phase takes place from day 0 to day 9 post-fracture followed by the reparative phase from day 9 to day 17 post-fracture. The remodeling phase started from 17 days onwards. At 25 days post-fracture, bone bridging is usually observed at the fracture site (Azuma et al, 2001, Einhorn, 1998, Ozaki et al, 2000, Sarisozen et al, 2002).

For fractures with other complication, for instance, in situation with neural damage demonstrated by sciatic nerve resection, the healing time would be prolonged. The inflammatory phase lasts until approximately 13 days after fracture. The reparative phase extends until day 28 post-fracture. The remodeling phase takes place from 28 days onwards (Madsen et al, 1998, 2000).

2.3 Low intensity pulsed ultrasound and fracture healing

2.3.1. Types and functions of ultrasound

Ultrasound is a form of mechanical energy that is transmitted through and into biological tissues as an acoustic pressure wave at frequencies beyond the human audible range (16-20 kHz) (Hajiargyrou et al, 1998). Ultrasounds delivered with different intensity are widely used in medicine for operative ($5-300\text{W}/\text{cm}^2$), therapeutic ($1-3\text{W}/\text{cm}^2$) or diagnostic ($1-50\text{mW}/\text{cm}^2$) purposes (Azuma et al, 2001, Hajiargyrou et al, 1998, Heckman, 1994, Pilla et al, 1990, Rubin et al, 2001). Low intensity (in the range of diagnostic use) pulsed ultrasound (LIPU) is a non-invasive, non-destructive and non-thermal physiotherapy modality used frequently in enhancing fracture healing (Hajiargyrou et al, 1998, Leung et al, 2004, Nolte et al, 2001) (Figure 4).

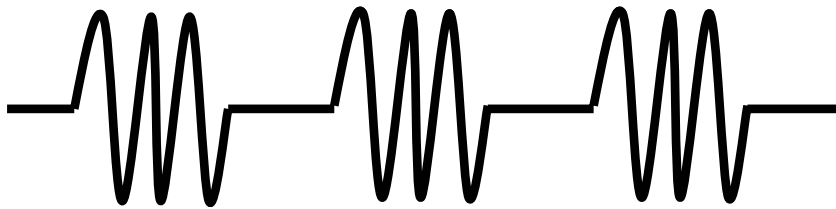


Figure 4 Typical waveform of pulsed ultrasound.

2.3.2. Physiological effects of ultrasound

It is believed that ultrasound interacts with the biological tissues by introducing a thermal change, cavitation and microstreaming. On passing through the tissue, the ultrasonic energy is absorbed at a rate proportional to the density of the tissue. The absorption of the ultrasound signal results in energy conversion to heat. This minor change in temperature ($<1^{\circ}\text{C}$) is enough to accelerate several enzymatic reactions in the tissues. Cavitation and microstreaming may mechanistically advance signal transduction pathways and modulate cell function (Hajiargyrou et al, 1998, Parvizi et al, 1999, Rubin et al, 2001, Wang et al, 1994, Warden, 2001).

2.3.3. Evidence of LIPU accelerating fracture healing

Clinical use of ultrasound to enhance fracture healing started as early as 1952 (Corradi & Cozzolino, 2001). Several studies have been performed to investigate the influence of LIPU on fresh fractures. In previous studies, LIPU has been found to improve several aspects of the healing process, including increasing bone mineral content, bone mineral density, peak torque, and stiffness, as well as accelerating the overall endochondral ossification process (Azuma et al, 2001, Ito et al, 2000, Jingushi et al, 1998, Takikawa et al, 2001). Animal studies performed on fresh fractures in rats and rabbits showed a mean acceleration of the healing process by 1.5 times (1.4 to 1.6 times in rats and 1.5 to 1.7 times in rabbits) in the LIPU treated group, as assessed by radiography and biomechanical testing (Pilla et al, 1990, Wang et al, 1994). Clinical studies on tibial diaphysis and distal radius indicated both that the period required to achieve clinical and radiological healing was

reduced by 38% in the LIPU treated group, and that treatment with LIPU was associated with decreased loss of reduction (Heckman et al, 1994, Kristiansen et al, 1997). The Food and Drug Administration (FDA) has approved the use of LIPU in enhancing the healing of fresh fractures (Rubin et al, 2001).

Apart from accelerating the healing of fresh fractures, LIPU has also been found to promote healing in delayed union and nonunion of fractures (Mayr et al, 2000, Takikawa et al, 2001, Nolte et al, 2001, Fujioka et al, 2000). Mayr et al (2000) applied LIPU in treating 951 delayed unions and 366 nonunions. They found that there was a 91% and 86% success rate for delayed unions and nonunions respectively. In a study performed by Yang & Park (2001), using canine ulna to investigate the effect of LIPU on moderate to large fracture gap, they discovered that LIPU could enhance new bone formation in small as well as large full-defect and at the same time, decrease the incidence of nonunion in the large defect model. Leung and his colleagues (2003) studied the effect of LIPU on fracture healing in more complicated fractures. In their study, they used LIPU to treat complex clinical tibial fractures. As with the simple fractures, statistically significantly better healing was found in the LIPU treated group. This indicates that LIPU could also accelerate healing in complicated fractures. It has also been demonstrated by several studies that LIPU could enhance fracture healing in less favorable conditions (e.g. in smokers and diabetes mellitus patients) (El-Mowafi & Mohsen, 2005, Gebauer et al, 2002, Heckman et al, 1994).

2.3.4. Effect of LIPU on different stages of fracture healing

Many research studies have been carried out to look at the effect of LIPU on different stages in the healing process. Azuma et al (2001), using a rat closed femoral fracture model, investigated the effect of timing and duration of LIPU treatment on fracture healing. The fracture sites received LIPU treatment at four different time periods (1-8 days, 9-16 days, 17-24 days and 1-24 days) and all the animals were sacrificed on day 25. Union was accelerated in the treated fractures in each group regardless of the duration of timing of the treatment. This implies that LIPU acts on each phase of the healing process.

Effect of LIPU on inflammatory phase

LIPU has been shown to induce a proinflammatory effect by greatly increasing the number of degranulated mast cells within the injured site in the inflammatory phase (Fyfe & Chahl, 1982, 1985). The whole healing process was speeded up by the early occurrence of the inflammatory effect. It has also been demonstrated that LIPU influences the influx of inflammatory cells, like macrophages, leukocytes and mast cells, which aids in earlier removal of the tissue debris in the inflammatory phase (Warden et al, 2000).

Effect of LIPU on reparative phase

LIPU has been found to accelerate callus formation in femur and fibular osteotomies in rabbits. In LIPU-treated osteotomies, callus formed during the first 10 to 12 days postinjury and stabilized in the days following, while in the control osteotomies, callus began to form at approximately 2 weeks postfracture (Duarte, 1983). This reveals that LIPU stimulates both the earlier commencement and completion of the fracture callus.

Effect of LIPU on chondrogenesis

Yang et al (1996) introduced LIPU at $50\text{mW}/\text{cm}^2$ during fracture repair and discovered that there was significantly earlier expression and earlier falls of genes coding for aggrecan, which were observed to be associated with chondrogenesis and endochondral ossification (Jingushi et al, 1992). This suggests that LIPU promotes earlier chondrogenesis and cartilage hypertrophy, resulting in the earlier onset of endochondral ossification. *In vitro* studies on chondrocyte populations using LIPU at the same intensity also suggest that LIPU increases chondrocyte expression of genes coding for aggrecan. This may have resulted from an enhanced uptake of calcium with LIPU exposure (Pavizi et al, 1997, Wu CC et al, 1996).

Effect of LIPU on osteogenesis

In differentiating cartilage and bone cell cultures, LIPU of 20-30mW/cm² has been shown to increase the bone cell uptake of calcium, modulate adenylate cyclase activity, and transforming growth factor beta (TGF-β) synthesis, bone morphogenetic protein (BMP) effects and parathyroid hormone (PTH) responses (Ryaby et al, 1989, 1992). Recently, Leung et al (2003) demonstrated the stimulatory effect of LIPU on human periosteal cells in the cellular differentiation and functional activation of bone formation. These findings address the promoting effect of LIPU on osteogenesis.

Effect of LIPU on blood flow and neovascularization

LIPU has been found to increase the degree of vascularity in an osteotomized dog ulna model of fracture healing during the late stages of the inflammatory phase and the reparative phase (Rawool et al, 2003).

Effect of LIPU on remodeling phase

Tanzer et al (1996) reported that LIPU stimulated bone ingrowth into porous coated dog femoral implants. In a clinical study done by El-Mowafi & Mohsen (2005), they found that LIPU stimulation has an accelerating effect on callus maturation during the consolidation phase in patients managed with tibial distraction osteogenesis. These two studies confirm the beneficial effect of LIPU on bone remodeling.

2.3.5. Efficacious signal parameters of LIPU

Many studies have been performed in an effort to define the most efficacious signal parameters. Wang et al (1994), in a study of bilateral femoral shaft fracture in rats, demonstrated that pulsed ultrasound with a 200 μ s burst of 1.5 or 0.5 MHz sine waves, repeated at 1 kHz, delivered at an intensity of 30mW/cm² for 15 minutes daily increased bone strength at the fracture site. Within 3 weeks, there was a 32% increase in stiffness of the femur that had been treated with 0.5 MHz (not significantly different from the control) and 67% increase in stiffness in the group treated with a 1.5 MHz burst (significantly greater than the control). Jingushi et al. (1998), using a femoral fracture model in rats to evaluate the pulse width and repetition frequency parameters of the ultrasound, discovered that a pulse width of 200 μ s was more effective in enhancing fracture healing than a pulse width of either 100 or 400 μ s, and that 1 kHz repetition was more osteoinductive than one of 2 kHz.

Despite those evidences suggesting the promoting effect of LIPU on fracture healing from animal and clinical studies, the exact physical mechanism of LIPU on fracture healing remains unknown. This may be due to the complex internal environment of the body. Previous experiments mainly focused on the ability of ultrasound to influence osteogenic cell activity and vascularity at the fracture site. There is still no general agreement on the exact physical mechanism of LIPU on fracture healing.

2.4 Bone innervation and fracture healing

Recently, it has been found that the peripheral nervous system, particularly neuropeptide-containing nerves, may play an important role in fracture healing and bone remodeling (Hukkanen et al, 1993, Konttinen et al, 1996, Madsen et al, 2000, Nordsletten et al, 1994, Onuoha, 2001, Onuoha & Alpar, 2000). In both human samples and animal models, the peripheral innervation was found to be decreased or absent in delayed union or non-union of diaphyseal fractures (Aro, 2001, Dyck et al, 1983, Zaidi, 1988). Femoral and sciatic nerve resection resulted in poor innervation as well as decreased stiffness and mineralization of the fracture callus (Garcia-Castellano et al, 2000, Madsen et al, 1998).

Innervation of bone was first reported in 1945 (Kuntz & Richins, 1945). Recent studies demonstrated in the rat that bone, callus and cartilage are innervated with neuropeptide-containing nerves, both in normal and pathological conditions (Hukkanen et al, 1993, Konttinen et al, 1996). Innervation of fracture callus was observed in rat tibia at 3 days postfracture, and the number of nerve fibers increased from day 14 to day 21 (Li et al, 2001). Hukkanen et al (1993) discovered that neuropeptide-immunoreactive nerves undergo changes in an ordered and sequential manner from 7 to 21 days of healing. Madsen et al. (1998) observed the effects of femoral and sciatic nerve resection on fracture healing and innervation of the fracture callus. At week 5 postfracture, neuropeptide-containing nerve fibers in the fracture callus were less and the stiffness of the callus was significantly lower in the

nerve resection group. Changes in neuropeptide-containing nerves in various pathological experimental situations imply that they are actively involved in local disease processes such as fracture healing (Garcia-Castellano et al, 2000, Hukkanen et al, 1993). These findings also suggest the important role of bone innervation on normal local bone turnover.

Peripheral innervation has been identified by several researchers as possessing nociceptive, mechanoreceptive and vasomotor functions (Aro et al, 1981, Thurston, 1982). The mechanoreceptive ability of the peripheral innervation may enable them to receive mechanical stimulus, like stress and strain, in the fracture site and respond to these mechanical stimuli by secreting neuropeptides, which in turn enhance fracture healing. Bone innervation may act as mechanoreceptors in biological tissues, sensing and responding to the mechanical stimuli generated by LIPU. Recently, a new term, “osseoperception”, describing the observation of the ability of patients with osseointegrated prosthesis to “feel” mechanical stimuli through their artificial limb, has been introduced (Klineberg & Murray, 1999, van Steenberghe, 2000, Ysander et al, 2001). One important finding from “osseoperception” is the active growth of small neuropeptides-containing nerve fibers at the bone-implant interface in a rat femoral model (Ysander et al, 2001). This suggests the hypothesis that the mechanical stimuli generated by LIPU are transferred into the body through peripheral innervation to regulate bone formation and remodeling in fracture healing.

Chapter 3 Objectives and Significance of The Study

LIPU transfers mechanical energy into tissues, thus it is important to relate the mechanical basis of ultrasound to the sensitivity of bone tissue through its sensory nerve fibers to mechanical stimuli. There was no report addressing this relationship. Thus the aim of this study was to investigate the role of bone innervation in response to LIPU for enhancing fracture healing. This aim was achieved by comparing the effects of LIPU on the healing of a standard three-point bending-induced tibial fracture with and without sciatic nerve resection in a rat model. The changes in size, bone mineral density and mechanical strength of the formed callus were evaluated and compared between each group.

With regards to the main objective of this study, the following hypotheses are proposed:

Alternative hypotheses:

1. The introduction of LIPU will significantly promote healing in fractures with nervous supply (i.e. the healing rate of the LIPU-treated fractures will be significantly faster than that of the sham LIPU-treated fractures in the presence of sciatic nerve).
2. Without nervous supply, the healing rate between the LIPU-treated and sham LIPU-treated fractures will be similar.

Null hypotheses:

1. The introduction of LIPU will not promote healing in fractures with nervous supply (i.e. the healing rate of the LIPU-treated fractures would be similar to that of the sham LIPU-treated fractures in the presence of sciatic nerve)
2. Without nervous supply, the healing rate between the LIPU-treated and sham-LIPU treated fractures will be different.

Injuries to the peripheral or central nervous system are common complications associated with fractures. It is estimated that 10% of fractures will require further surgical procedures because of impaired healing (Bonnarens & Einhorn, 1984). LIPU is an effective physiotherapy modality for enhancing fracture healing generally, but its effect on the healing of fractures accompanied with neural complications has not been explored. Up to now, there is no report addressing the relationship between neuropeptide-containing nerve fibers and LIPU. The present study will provide a basis for this.

Chapter 4 Methodology

4.1 Animal model

One hundred and twenty mature female Sprague-Dawley rats with mean weight of 261.44g (range 218.8 – 298.7g) at 12 weeks of age were used for this study. All the animals were mixed breeds and were obtained from the Centralized Animal Facilities (CAF) of the Hong Kong Polytechnic University.

4.2 Ethical considerations

This study was approved by the Ethics Committee of the Hong Kong Polytechnic University (Appendix I), and a license to conduct animal experiments was also issued by the Department of Health of Hong Kong (Appendix II).

4.3 Study design

Closed transverse diaphyseal fracture models were created on the right tibia on all the animals in this study. Animals were assigned randomly into 4 groups; the sham LIPU neural intact group (Group I), the LIPU neural intact group (Group II), the sham LIPU neurectomy group (Group III) and the LIPU neurectomy group (Group

IV). Different treatments were given to animals in different group as illustrated in Table 1. Animals in the two LIPU treatment groups (II and IV) received a daily LIPU treatment at the fracture site starting at day 2 after fracture (post-operation day 1). The sciatic nerve of the fractured leg (in this experiment, the right tibia) was dissected in those animals assigned to the two neurectomy groups (III and IV).

To overcome the problem of unequal load bearing between animals in the neural intact and those in the nerve resection groups, patella tenotomy was performed on animals in the two neural intact groups (I and II). It has been demonstrated by a previous study on inducing disuse osteopenia (Kimmel et al, 1999) that tenotomy of the patella tendon could create a similar effect of immobilization to sciatic neurectomy.

Animals were sacrificed for tissue analysis and bone mechanical testing at days 7, 14 and 21 post-fracture accordingly (Table 2).

Table 1. Treatments on different groups

Group	Treatment		
	Ultrasound Treatment	Nerve Resection	Patella Tenotomy
I: Sham LIPU neural intact group (n=33)	No	No	Yes
II: LIPU neural intact group (n=34)	Yes	No	Yes
III: Sham LIPU neurectomy group (n=27)	No	Yes	No
IV: LIPU neurectomy group (n=26)	Yes	Yes	No

Table 2. Evaluation Methods

Evaluation Methods	Day of sampling after surgery
◆ Radiographic evaluation, bone densitometry, and mechanical testing	21
◆ Histomorphometry	7
	14
	21

4.4. Surgical Procedures

4.4.1. Tibial fracture model

The closed transverse diaphyseal fracture model standardized by Bonnarens and Einhorn (1984) was used in this study. Surgery was performed under sterile conditions and under general anesthesia by intraperitoneal injection of chloral hydrate (Fluka, Switzerland) (1ml/100g). Through a 1cm longitudinal incision, the medial tibial condyle just below the medial part of the knee joint was exposed. With the use of a surgical drill, a hole 3mm in diameter was created. A 21-gauge needle was inserted into the medullary canal. The soft tissue and the skin were closed with resorbable sutures. The stabilized tibia was then placed in a three-point bending device, and the diaphysis of the fixed tibia was fractured at mid shaft by the force of a 500g weight dropped from 35cm (Figure 5, 6).

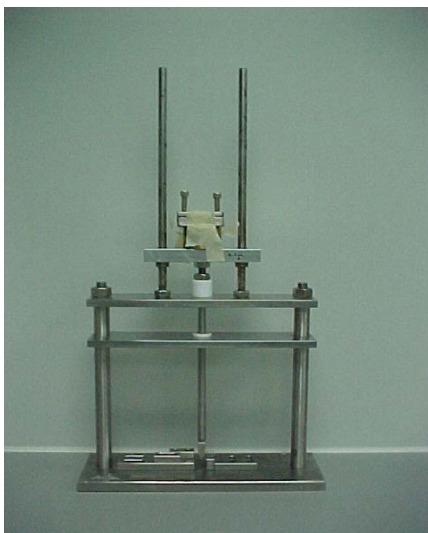


Figure 5 A device for creating fracture.



Figure 6 Fracture creating method.

Fractures outside the central 8mm portion and other types of fractures (around 15% according to our pilot study) were excluded from the study. Animals were then randomly assigned to different experimental groups. Lateral tibial radiographs were taken after the surgery and at the end of the experiment, in order to evaluate the position and orientation of each fracture (Figure 7).

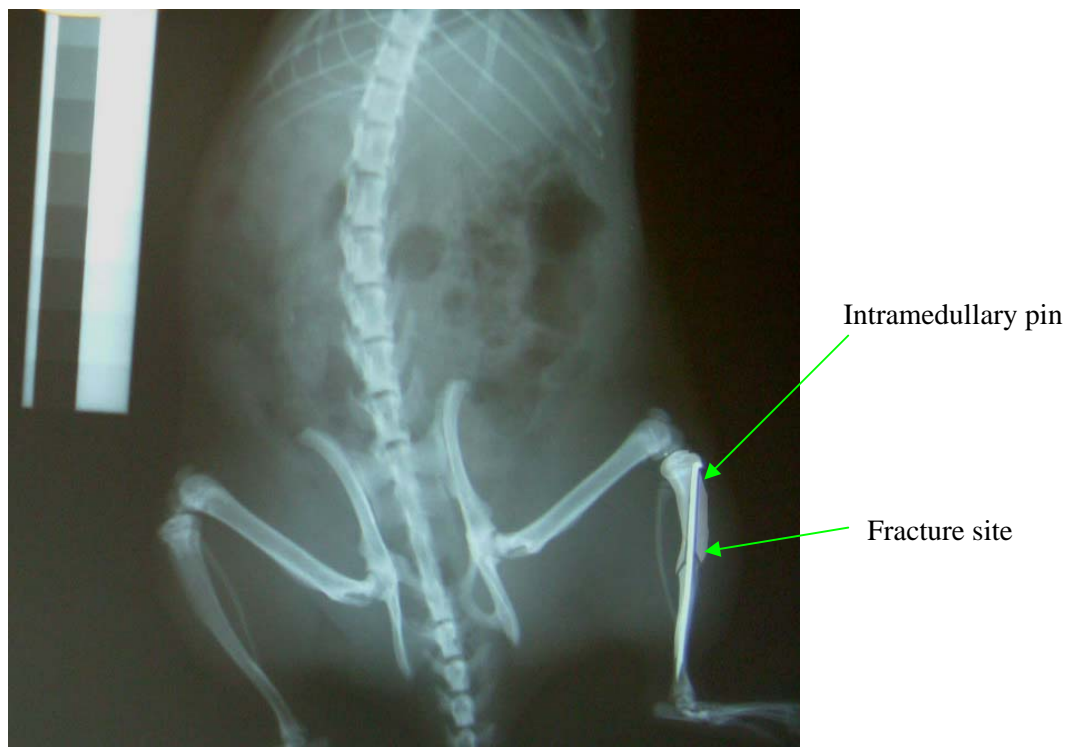


Figure 7 Lateral tibial radiograph for evaluating the position and orientation of the fracture.

4.4.2 Resection of sciatic nerve

The sciatic nerve of the fractured leg was dissected in animals assigned to the nerve resection groups. The method described by Madsen et al (2000) was used. A 5mm section of the sciatic nerve was dissected through a 1 cm skin incision over the lateral upper part of the thigh (Figure 8).



Figure 8 Surgical resection of sciatic nerve.

4.4.3. Resection of the patella tendon

The patella tendon of the fractured leg was dissected on those animals assigned to the two neural intact groups. A longitudinal incision was made on the antero-medial aspect of the right knee and the patella tendon was identified by blunt dissection with a probe. A 5mm section of the patella tendon was then transected (Figure 9).

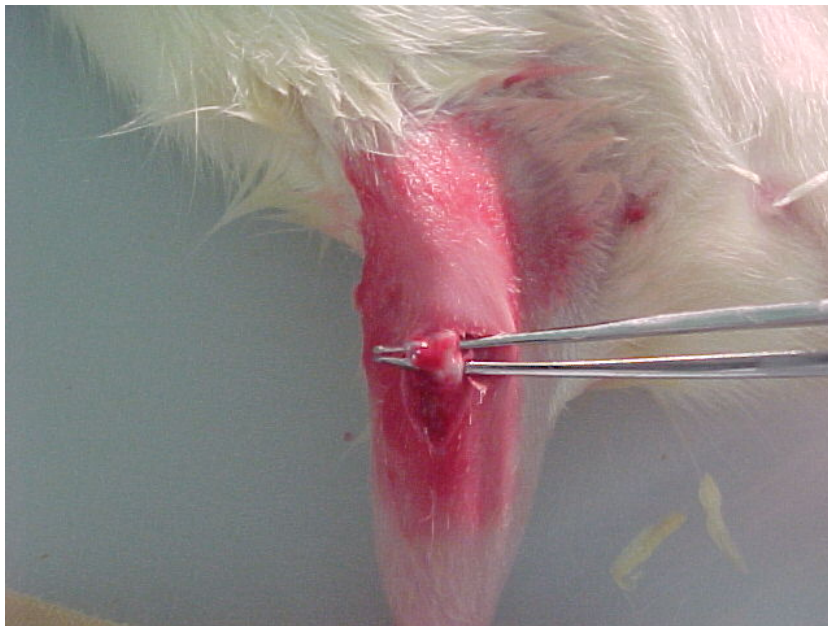
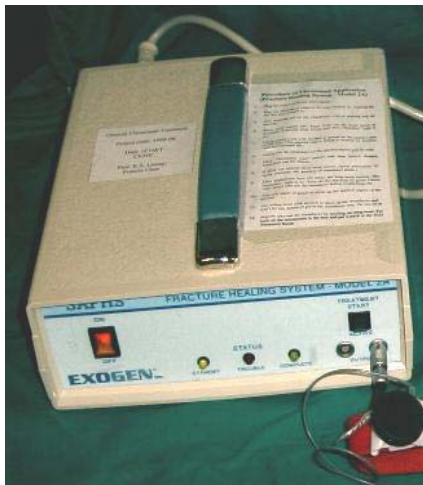


Figure 9 Surgical resection of patella tendon.

After the surgery, animals were kept in individual wire-topped plastic cages in a room with a 12-hour light and 12-hour dark cycle. They were allowed unrestricted ambulation in their cages. Water and food were given *ad libitum* throughout the whole period.

4.4.4. LIPU treatment

Under general anaesthesia by intraperitoneal injection of chloral hydrate (1mg/100g), the fracture site received daily a LIPU or sham exposure for 15 minutes (Leung, 2001). LIPU was delivered by a 2.5cm diameter ultrasound transducer (SAFHS, Exogen, Inc, West Caldwell, NJ, USA) placed against the lateral surface of the fracture site/ mid shaft of the tibia with the characteristics illustrated in Figure 10. Ultrasound gel (Other-Sonic Generic Ultrasound Transmission Gel, Pharmaceutical Innovations, USA) was used as the coupling mediator between ultrasound transducer and skin. Application of LIPU/ sham treatment started on the 2nd day after the fracture was created.



Frequency	1.5MHz
Wave shape	Sine wave
Signal type	Pulsed
Length of signal	200µs
Off period	800µs
Repetition	1kHz
Intensity	30 mW/cm ²

Figure 10 Specifications of ultrasound machine (SAFHS, Exogen Inc, NJ, USA).

4.5 Outcome evaluation

4.5.1. Radiographic evaluation

Plain lateral radiographs were taken on the operated limb for each animal at post-operation day 1 and at the end of the experiment (i.e. post-operation days 7, 14 and 21 according to the group the animal belonged to) with the use of a Faxitron X-ray machine (Model 43855C, Wheeling, IL, USA) at 60 kV for 5 seconds. The films were processed using an automatic X-ray developer (Okamoto X3, Okamoto Manufacturing Co. Ltd., Taiwan).

The diameters of the original bone shaft at the same level as fracture created on the fractured limb (D1) and the maximum diameter of the callus (D2) were measured for all the animals by two different assessors (three times for each parameter by each assessor) from the X-ray taken at post-operation day 21 with an image analysis software (ImageJ 1.29x, Wayne Rasband, National Institutes of Health, USA). In measuring the diameter of the callus, a line that is parallel to the limb was drawn. The maximum width of the callus, which is perpendicular to the tibia, was then measured. The callus index was recorded according to the averaged D2 to D1 ratio.

Fracture union rate was also evaluated on each animal by two different assessors from X-rays taken at 21 days post-operation.

4.5.2 Bone densitometry

After removal of the soft tissues and intramedullary nail, the mineral density of the fracture callus was determined for animals in all the groups at post-operation day 21 using a high resolution and multi-slice peripheral quantitative computed tomography (XCT 2000, Norland Stratec, Germany) (Figure 11). Specimens were put into a plastic tube during the whole process. Both the fractured tibia and its contralateral tibia were scanned together. Altogether 3 non-consecutive 1-mm-thick slices, each of 5mm apart, were scanned from the transverse plane of the tibia and located with the 2th slice at the fracture site (Figure 12 & 13). The threshold values were set at 269mg/cm³ and 711mg/cm³ for trabecular and cortical bone respectively. The volumetric bone mineral density (BMD), the bone mineral content (BMC), and the cross-sectional area (BA) were analyzed by using a manufacturer-supplied software program (Blokhuis et al, 2000, Cheng et al, 2000, Leung, 2001, Qin et al, 1997). The precision error of the pQCT operation to measure the total density of the bone (including repositioning of the specimens and independent analyses) was 0.38% with a standard resolution of 0.5mm.



Figure 11 XCT 2000, Norland Stratec, Germany

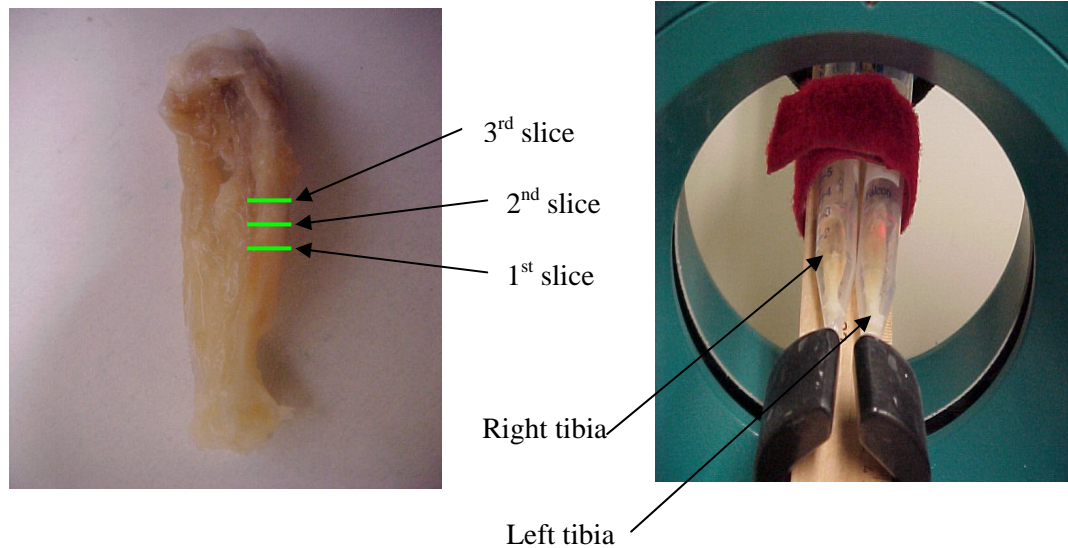


Figure 12 Position of each slice for scanning

Figure 13 Data retrieval by the machine

4.5.3. Mechanical testing

After the pQCT measurement, a four-point bending test was conducted on bilateral tibiae for those animals assigned for mechanical testing using a Hounsfield Material Testing Machine (model H10KM, Hounsfield Test Equipment, UK) with a 1000N load cell (Figure 14). Specimens were wrapped by gauze soaked with 0.9% saline and stored at -20°C. They were thawed at room temperature a few hours before the mechanical testing. A constant span length of 20mm was set between the two lower supports for each specimen. The tibia was positioned horizontally with the anterior surface downward, centered on the supports, and the pressing force was directed vertically to the midshaft of the bone (Figure 15). Loading was applied at a constant speed of 2mm/min until failure (Bak B, 1988 & 1992). A slow load rate (2mm/min) but not a fast load rate was used in the mechanical measurement so as to demonstrate the bone elasticity. In order to minimize the effect of deep freezing that might be introduced to the specimen, each specimen was pre-conditioned with 5 oscillation cycles of a pre-load (20 and 50N for fractured limb and contralateral limb respectively) at a constant rate of 2mm/min. Saline was sprayed on the specimens during testing to avoid dehydration. All the data were measured and recorded by the computer system that was connected to the mechanical testing machine. The load-displacement curve generated by the computer system was used for analysis. The ultimate load was defined as the bending load at failure (Jamsa, 2000, Utvag et al, 1998 Utvag & Reikeras, 1998, Volkman, 2004). Stiffness was calculated as the slope of the linear region between 20 to 70% of the maximum load from the load-displacement curve (Utvag et al, 1998, Utvag & Reikeras, 1998)

(Figure 16). The coefficient of variation for the ultimate load as well as stiffness performed on ten trials was 10% and 26% respectively.

The union rate was also recorded by counting the numbers of unbroken tibiae to the total numbers of tibiae in each group during pin removal before mechanical testing.

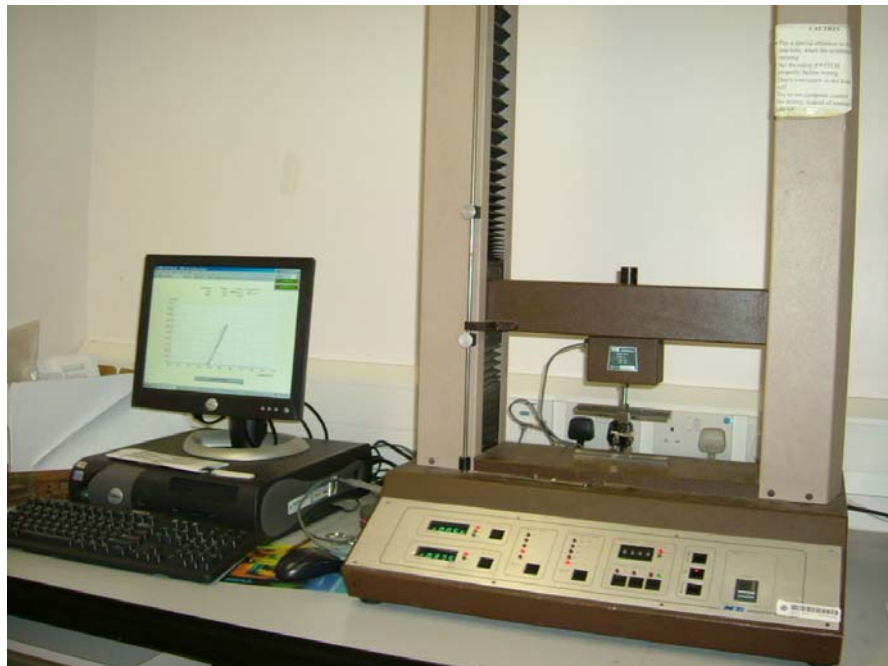


Figure 14 Hounsfield Material Testing Machine (H10KM, Hounsfield Test Equipment, UK) with a 1000N load cell

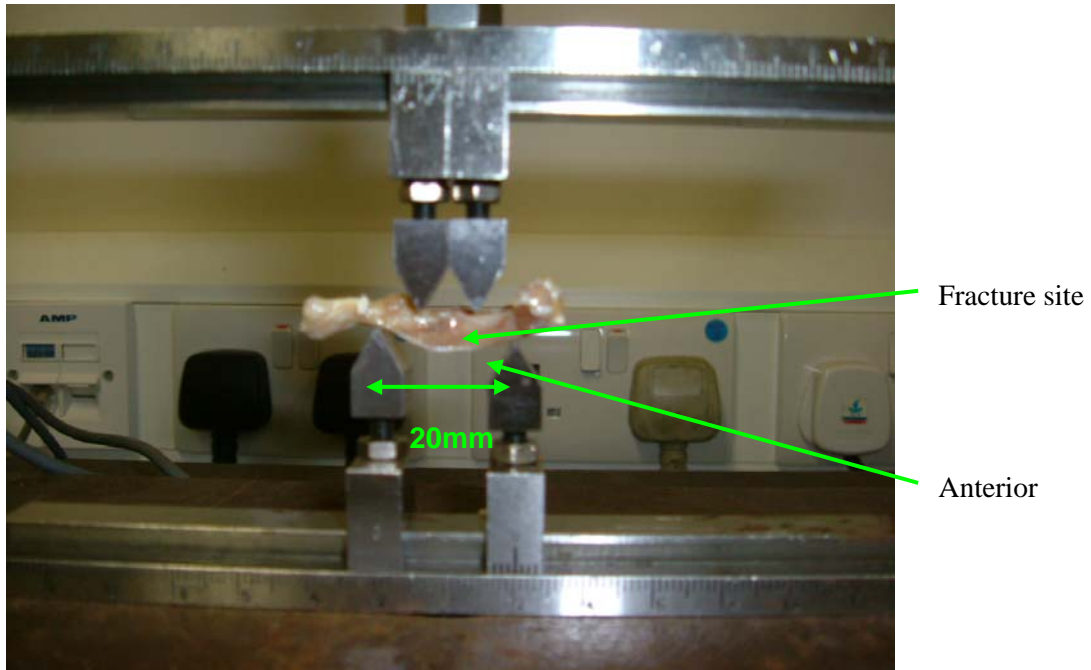


Figure 15 Set up and orientation of the specimen for four-point bending test.

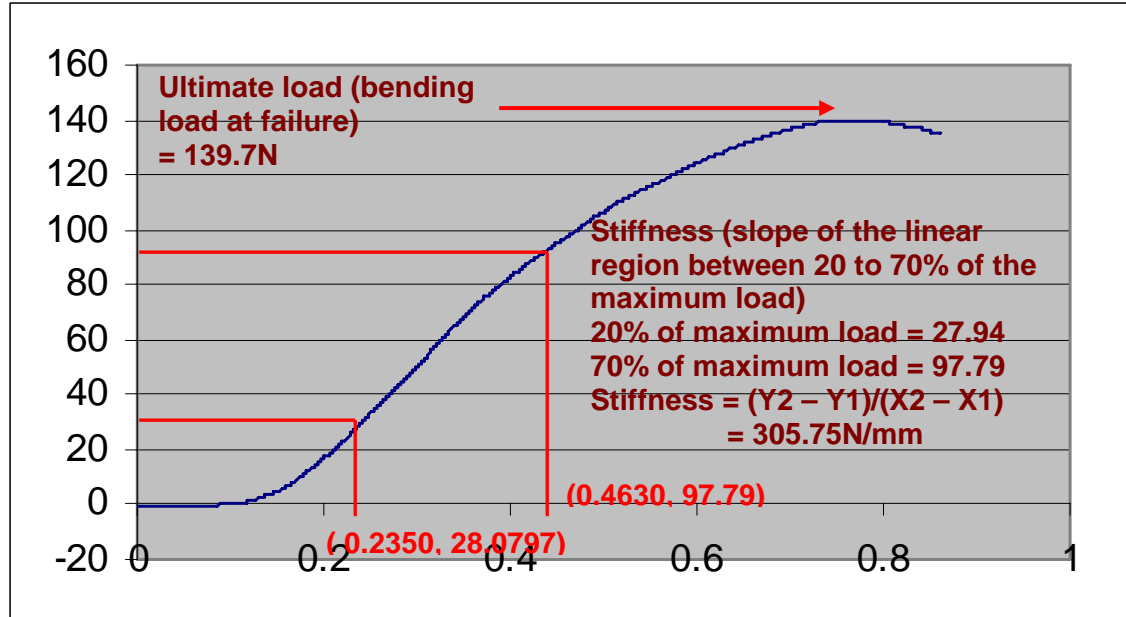


Figure 16 Load-displacement curve generated by the computer system of the mechanical testing machine

4.5.4. Histomorphometry

At the end of the experiment, the animals were anesthetized and perfused with a total of 300ml of normal saline followed by 4% phosphate buffered paraformaldehyde *in vivo* via cannulation of the ascending aorta through the left cardiac ventricle (Guo, 1994, Hukkanen et al, 1995). The tibia was removed and cleaned of all soft tissues, with care taken to preserve the periosteum around the fracture callus. The bone was immersed in 4% phosphate buffered paraformaldehyde at 4°C overnight, then decalcified with 10% ethylenediaminetetraacetic acid (EDTA) for 3 to 4 weeks. Specimens were put into tissue cassettes and underwent a series of processes of dehydration with graded ethanols, clearing with xylene and finally embedded in paraffin wax with the use of an automatic tissue processor (Shadon, England) (Figure 17). Paraffin sections 8µm in thickness were cut parallel to the longitudinal axis, with the central section being in the center of the specimen, by using a semi-motorized rotary microtome (RM2145, Leica, Germany). Sections were stained with Haematoxylin and Eosin (H&E). Tissue morphology was assessed on the H&E stained sections.



Figure 17 Tissue Processor (Shadon, England).

4.6 Statistical analysis

The Statistical Package for Social Science (SPSS) for Microsoft Windows version 11.5 was employed for data analysis in this study. An α level of 0.05 was set for all the statistical comparisons. Reliability was tested by calculating the Intraclass Correlation Coefficients (ICC) for those parameters measured by two different assessors. The primary analysis was to determine the effect of LIPU on fracture healing and callus innervation in fractures with and without neural damage. Intra-group comparison of the measurements, including differences in callus index, bone mineral density (BMD), mechanical properties and bone structure as well as immunohistological variables of the callus region such as degree of callus innervation as described above were performed between the treated fracture and the sham-treated fracture. The hypotheses were tested with the use of two-way ANOVA. Bonferroni's multiple comparison test was used to identify statistically significant differences among groups and at each healing time point. Pearson's correlation coefficient was used for calculating the relationship between the callus index from the x-ray, with the callus area measured by pQCT, and ultimate load and stiffness from mechanical testing with bone mineral density (BMD), bone area (BA) and bone mineral content (BMC) from pQCT measurement.

Chapter 5 Results

5.1. Radiographic evaluation

Radiographic evaluation was performed by calculating the callus index (D2 to D1 ratio) and counting the union rate from the lateral radiograph of the fractured tibia taken at 21 days post-fracture. Table 3 lists the distribution of animals in each treatment group.

As mentioned, in calculating the callus index, the D1 (diameter of the original bone shaft) and D2 (diameter of the callus) values were recorded by two assessors. The intra-class correlation coefficient (ICC) was 0.8174, $p=0.000$ after averaging the results between the two assessors. (The inter-rater reliability was good when the $ICC \geq 0.75$) (Portney & Watkins, 2000). Table 4 shows the results of the ICC between the two raters.

5.1.1. Callus index

The results on the callus index in each treatment group are shown in Table 5. The results of two-way ANOVA reveal that there was a significant main effect of nerve resection on the callus index ($p=0.002$) (Figure 18). Larger callus size was found on those groups with nerve resection.

5.1.2. Union rate

The results on union rate evaluated from X-ray are listed in Figure 19. The highest union rate was found in the LIPU neural intact group (72%). A higher union rate was found in the LIPU-treated group when comparing between the two neural intact groups. For the two neurectomy groups (with or without LIPU treatment), the same union rate (52%) was found.

Table 3. Distribution of animals for radiographic evaluation in different groups

Treatment	No. of animals
Sham LIPU neural intact	21
LIPU neural intact	22
Sham LIPU neurectomy	23
LIPU neurectomy	25
Total	91

Table 4. Results of intra-class correlation coefficients (ICC) between the two assessors (n = 91)

Measure	ICC value	95% confidence interval		F value	Sig.
		Lower bound	Upper bound		
Single rater	0.6912	0.5513	0.7904	5.9078	0.000
Average of raters	0.8174	0.7074	0.8838	5.9078	0.000

$\alpha=0.8307$

Table 5. Results of callus index in each treatment group

Treatment	Callus Index (D2/D1)
Sham LIPU neural intact	1.05 ± 0.11
LIPU neural intact	1.04 ± 0.08
Sham LIPU neurectomy	1.13 ± 0.16
LIPU neurectomy	1.15 ± 0.19

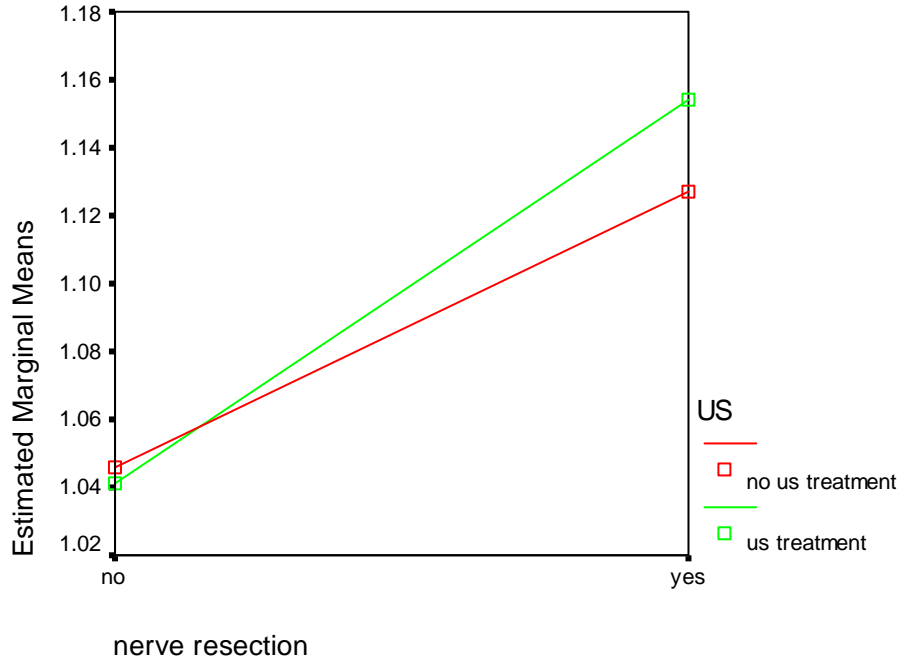


Figure 18 Results of two-way ANOVA for callus index

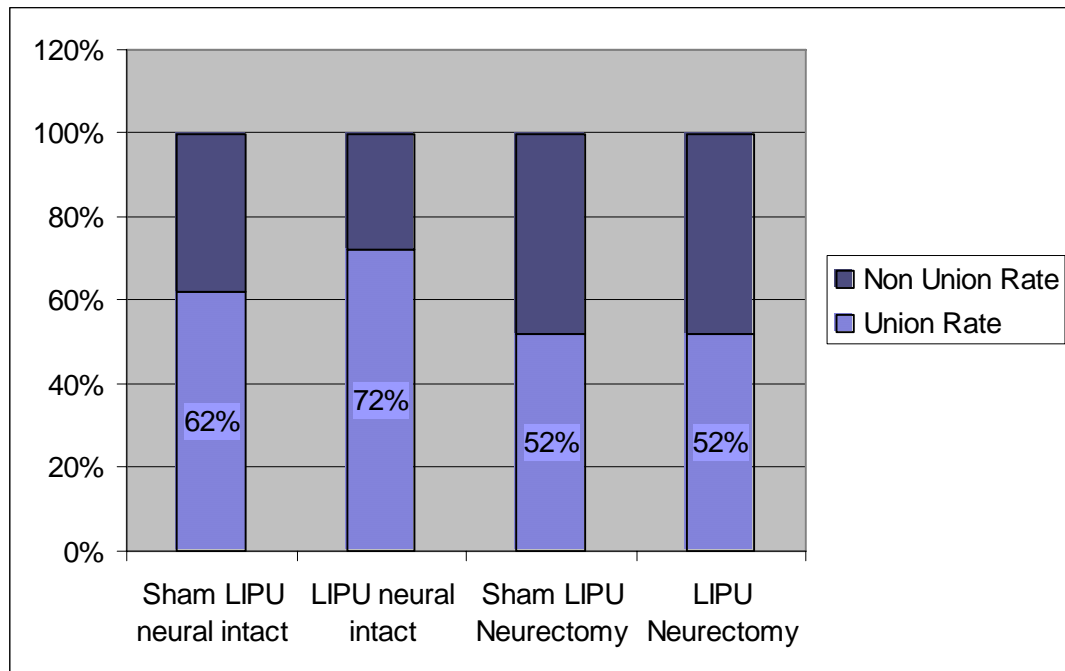


Figure 19 Results on union rate evaluated from x-ray in each treatment group

5.2. Densitometry by pQCT

The total BMD, total BMC and total BA were studied by pQCT on animals at 21 days post-operation. The right tibiae on 10 of the animals were broken during pin removal before pQCT measurement. Therefore, pQCT measurement could not be performed on these 10 animals. Altogether 81 animals were scanned with the pQCT machine. The distribution of animals is listed in Table 6.

5.2.1. Total BMD

Table 6 shows the results on total BMD assessed by pQCT in each treatment group. The results of two-way ANOVA (as shown in Figure 20) indicate a significant interaction ($p=0.045$) between the two factors (innervation and LIPU) on total BMD. The results of Bonferroni's multiple comparison test (Table 7) reveal that with the presence of the sciatic nerve (i.e. no nerve resection), the introduction of LIPU could significantly increase the total BMD in the fractured callus ($p=0.005$). However, such increase in total BMD, caused by the introduction of LIPU, was not found while the sciatic nerve was absent (i.e. with nerve resection).

Table 6. Results obtained from pQCT measurements in each treatment group

Treatment	N	Total BMD (mg/cm ³)	Total BMC (mg)	Total BA (mm ²)
Sham LIPU neural intact	20	654.81 ± 81.43	8.56 ± 1.94	13.32 ± 3.80
LIPU neural intact	19	703.67 ± 92.05	8.24 ± 1.82	11.88 ± 2.96
Sham LIPU neurectomy	19	637.91 ± 104.56	8.52 ± 2.15	13.69 ± 4.19
LIPU neurectomy	23	638.12 ± 95.55	8.34 ± 2.31	13.71 ± 6.00

Table 7. Results of Bonferroni's multiple comparison test for total BMD

	(I) US	(J) US	Mean Difference		
	treatment	treatment	(I-J)	SE	Sig.(a)
Nerve resection	No	Yes	-48.862(*)	17.332	.005
	Yes	No	48.862(*)	17.332	.005
	No	Yes	-.208	16.773	.990
	Yes	No	.208	16.773	.990

Dependent variable: Total density right

Based on estimated marginal means

*: The mean difference is significant at the .05 level.

a: Adjustment for multiple comparisons: Bonferroni.

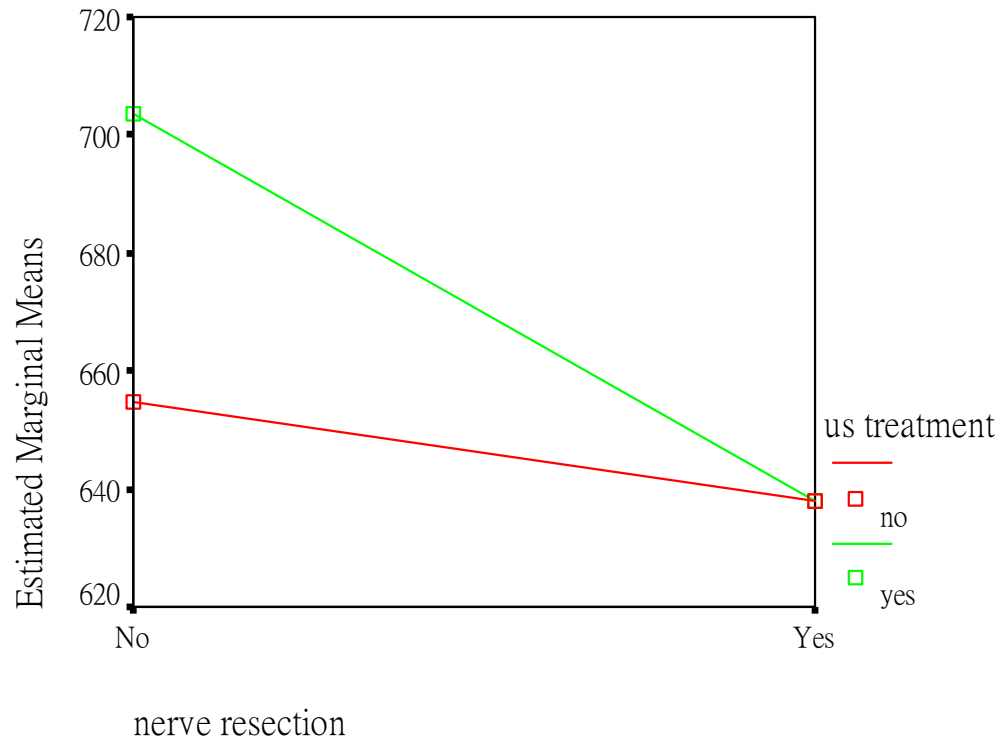


Figure 20 Results of two-way ANOVA for total BMD assessed by pQCT

5.2.2. Total BMC

The results on total BMC, measured by pQCT in each treatment group, are listed in Table 6. No significant main effect was found from the two factors (innervation and LIPU) on total BMC by using two-way ANOVA (Figure 21).

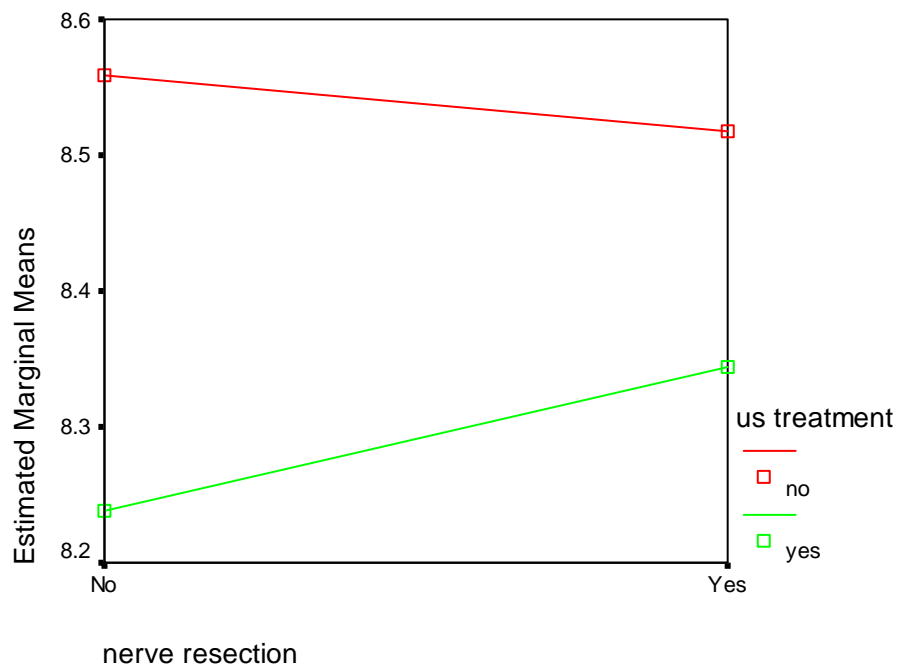


Figure 21 Results of two-way ANOVA for total BMC assessed by pQCT

5.2.3. Total BA

Table 6 lists the results on total bone area (BA) in each treatment group assessed by pQCT. The smallest total BA was found on the LIPU neural intact group (11.88mm^2); however, similar to total BMC, no significant main effect was found from the two factors (innervation and LIPU) on total BA by using two-way ANOVA (Figure 22).

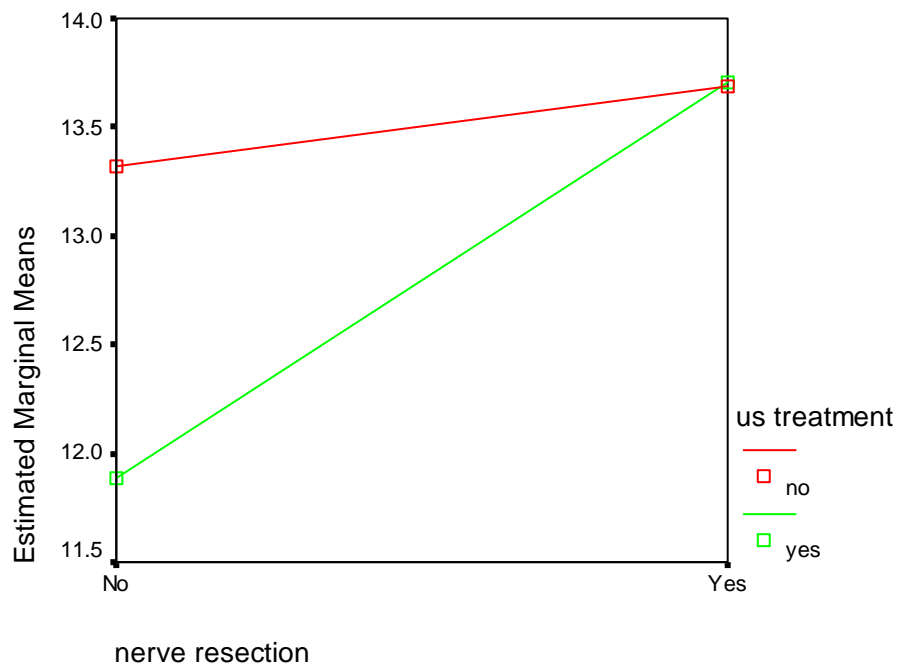


Figure 22 Results of two-way ANOVA for total BA assessed by pQCT

5.3. Mechanical testing

Altogether 35 animals were prepared for mechanical testing. Eleven of them were excluded because the tibiae were broken during pin removal before the four-point bending test. The test was only performed on 24 animals. Table 8 lists the distribution of animals in each treatment group.

5.3.1. Ultimate load from four-point bending test

Table 8 indicates the results on ultimate load from the four-point bending test in each treatment group. No significant main effect could be found from the two factors (innervation and LIPU) on ultimate load from two-way ANOVA (Figure 23).

Table 8. Results on ultimate load and stiffness obtained from four-point bending test in each treatment group

Treatment	N	Ultimate Load (N)	Stiffness (N/mm)
Sham LIPU neural intact	6	46.42 ± 34.77	147.27 ± 129.78
LIPU neural intact	8	33.91 ± 33.21	115.38 ± 96.79
Sham LIPU neurectomy	5	39.39 ± 30.45	103.68 ± 85.43
LIPU neurectomy	5	31.73 ± 21.61	84.57 ± 75.76

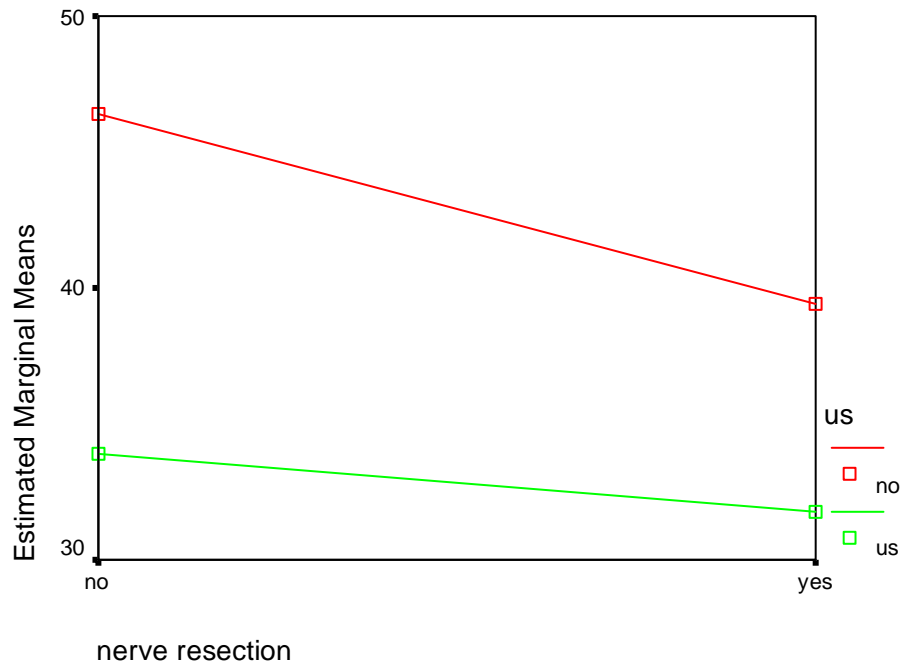


Figure 23 Results on two-way ANOVA for ultimate load

5.3.2. Stiffness from four-point bending test

The results on stiffness from the four-point bending test in each treatment group are listed in Table 8. Similar to ultimate load, no significant main effect was found from the two factors (innervation and LIPU) by two-way ANOVA (Figure 24).

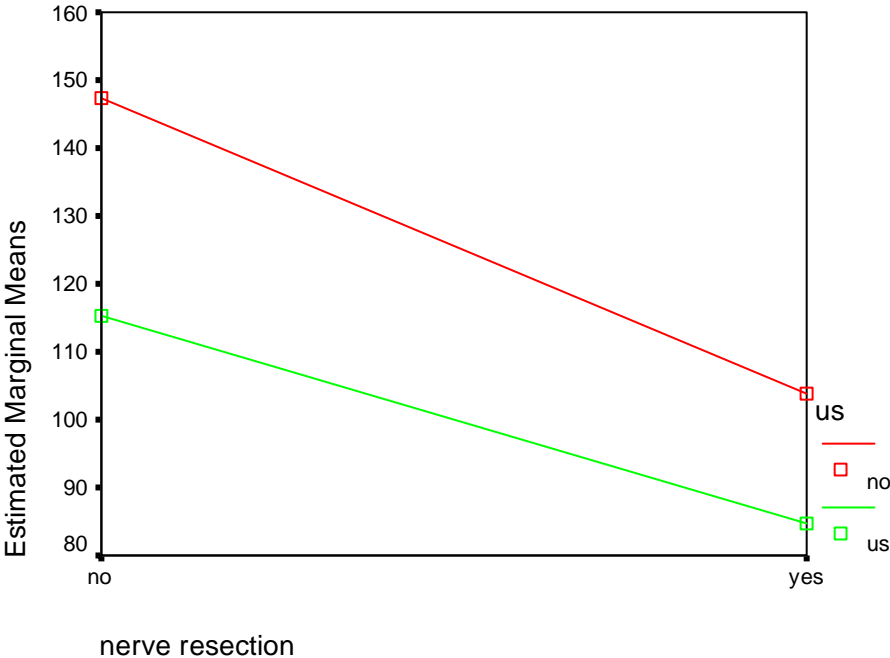


Figure 24 Results on two-way anova for stiffness

5.3.3. Union rate assessed during pin removal

Union rate was assessed from 35 animals that were prepared for mechanical testing by counting the numbers of unbroken tibiae during pin removal in each treatment group. Results are listed in Figure 25. The highest union rates were found in the LIPU neural intact group (89%), followed by the sham LIPU neural intact group (75%). The lowest union rates were found in the two neurectomy groups (both were 56%). These were similar to findings on union rates evaluated by radiograph.

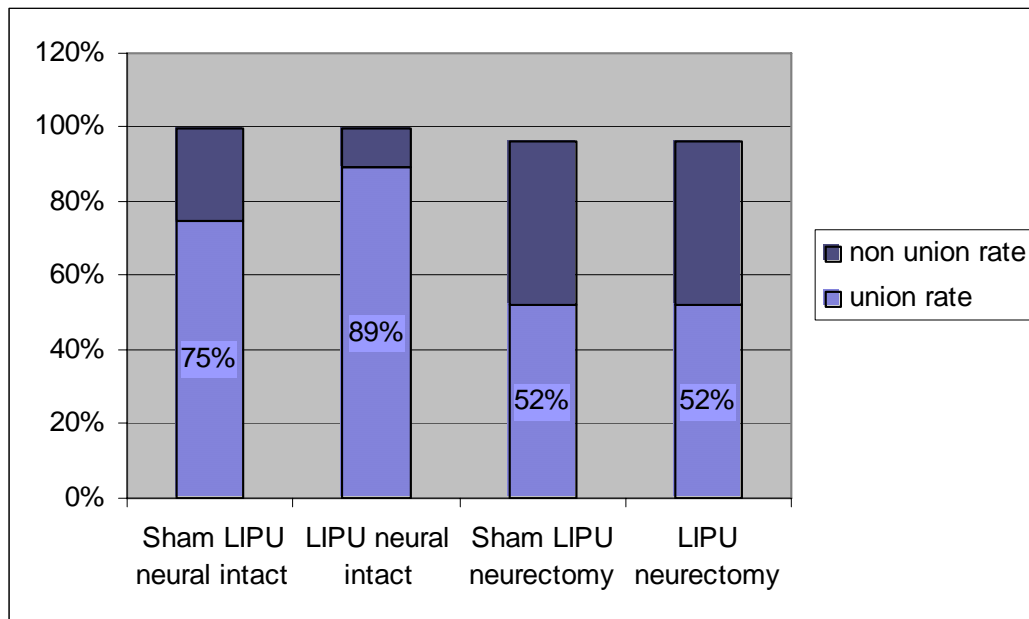


Figure 25 Results on union rate obtained during pin removal before four-point bending test in each treatment group

5.4. Correlations

5.4.1 Correlations between callus size evaluated by radiograph and pQCT

Significant correlations were found between the callus index evaluated by radiograph and the area measured by pQCT ($p=0.008$). Results also revealed that there was a fair degree of relationship ($r=0.291$) between the two parameters (correlations from 0.25 to 0.50 suggest a fair degree of relationship) (Portney & Watkins, 2000).

5.4.2. Correlations between bone strength-related parameters obtained from pQCT and those from four-point bending test

The results of correlations between total bone mineral density (BMD), total bone mineral content (BMC) and total bone area (BA) from pQCT with ultimate load and stiffness obtained by four-point bending test are showed in Table 9. No significant correlations were found between any of the parameters.

Table 9. Correlations between bone strength-related parameters obtained from pQCT and those from four-point bending test

		Total BMD	Total BA	Total BMC	SSI polar	SSIx	SSIy
Ultimate load	Pearson Correlation	-.200	.212	.161	.064	-.157	.132
	Sig. (2-tailed)	.348	.321	.451	.765	.464	.540
	N	24	24	24	24	24	24
Stiffness	Pearson Correlation	-.236	-.027	-.104	-.048	-.226	.007
	Sig. (2-tailed)	.266	.902	.628	.823	.288	.972
	N	24	24	24	24	24	24

5.5. Histomorphometry

The results of H&E stained sections from 7, 14 and 21 days post-fracture show that the fracture callus gradually matures from 7 to 21 days post-fracture (Figure 26-37, magnification was set at 100x). At day 7 post-fracture, the callus was mainly filled with fibrous tissue. Mixtures of cartilage, woven and lamella bone was found in the fracture callus one week later. At day 21 post-fracture, the area of cartilage in the fracture callus was reduced and replaced by lamella bone. However, the rate of maturation/healing of the fracture callus was slightly different between the different treatment groups. When comparing the H&E stained sections from different treatment groups, a more mature callus was found in the groups with intact sciatic nerves. This was indicated by the presence of cartilage, woven and lamella bone (more mature bone types) in the fracture callus at 14 days post-fracture in the neural intact groups, while mainly fibrous tissue was found in the fracture callus from the neurectomy groups. At 21 days post-fracture, a large amount of cartilage was reduced, leaving mainly woven and lamellar bone in the fracture callus in the groups with intact nerves, while large amounts of cartilage still appeared in the neurectomy groups. Again, this suggests that the fracture callus in groups with intact nerves healed faster and better than in those without.

The results on the H&E stained sections also revealed that in the neural intact groups, the introduction of LIPU could increase the rate of maturation/healing of the fracture callus. At 21 days post-fracture, comparing the two neural intact groups, the

fracture callus treated with LIPU was mainly filled with lamellar bone, while mixtures of woven and lamellar bone were found in the group treated with sham LIPU. However, the promoting effect of LIPU on the healing of the fracture callus was not seen in the absence of the sciatic nerve. This was indicated by the presence of similar bone types in the fracture callus in the two groups with nerve resection at 21 days post-fracture.

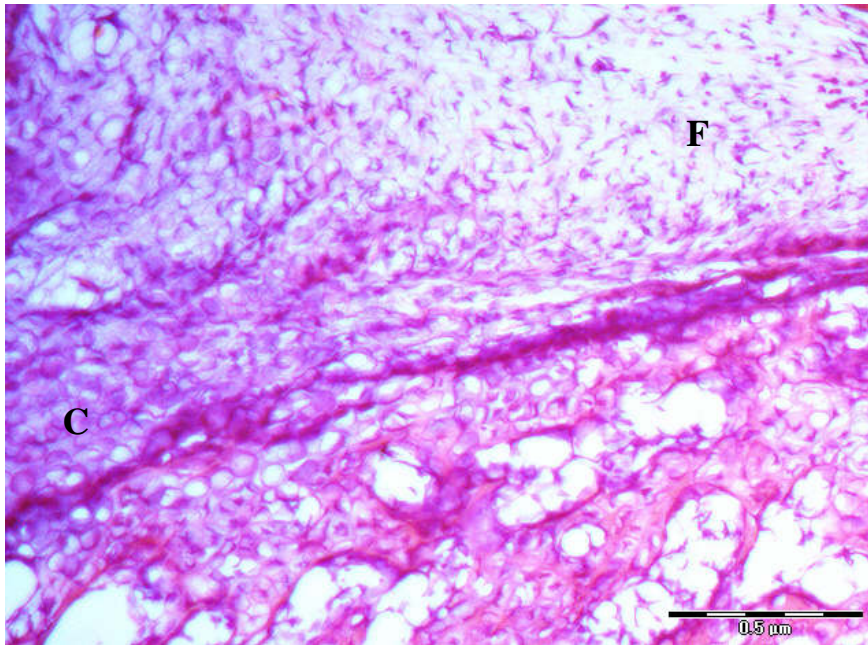


Figure 26 Sham LIPU neural intact group at 7 days post-fracture (H&E, 100x)
Fibrous tissue (**F**) and small amount of cartilage (**C**) were found in the fracture site

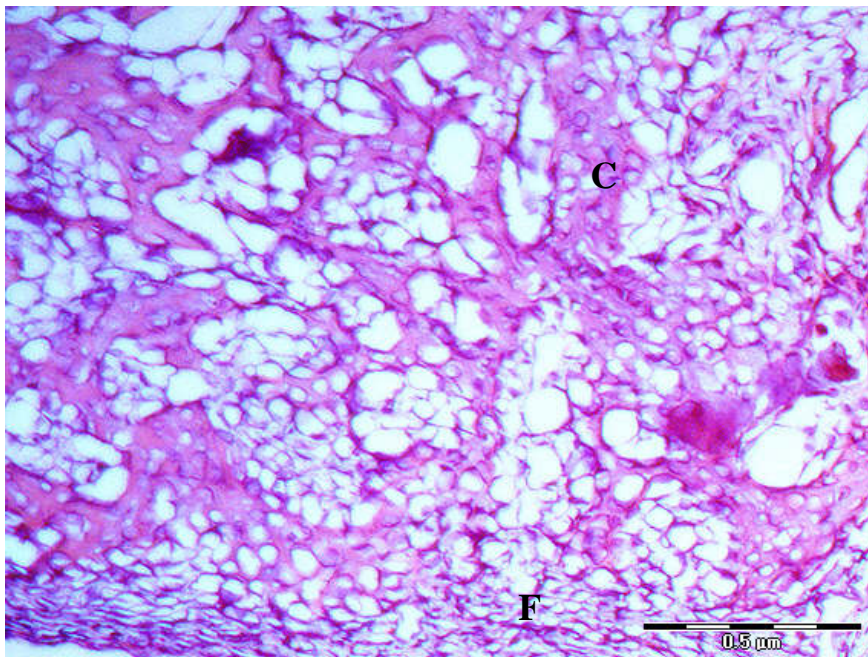


Figure 27 LIPU neural intact group at 7 days post-fracture (H&E, 100x)
Mixture of fibrous tissue (**F**) and cartilage (**C**) were found in the fracture site

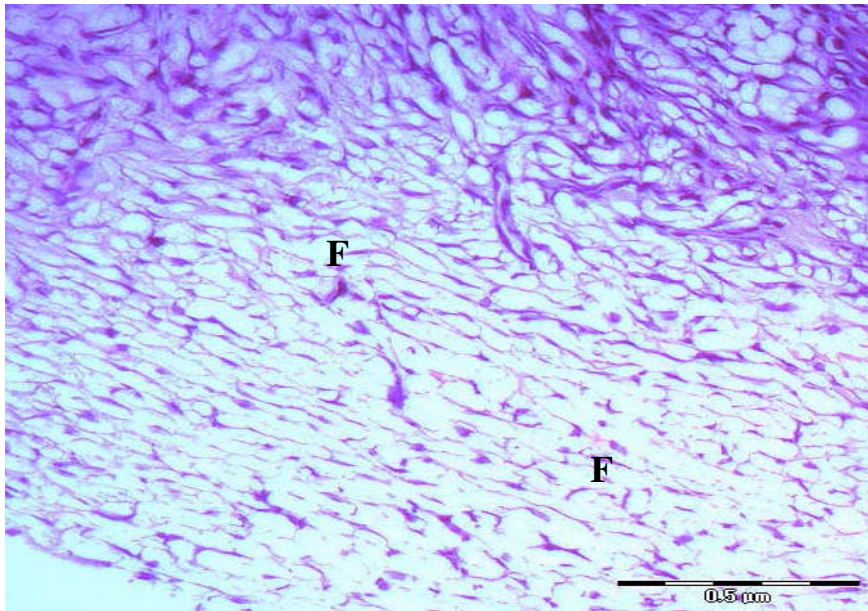


Figure 28 sham LIPU neurectomy group at 7 days post-fracture (H&E, 100x)
Fibrous tissue (**F**) was mainly found in the fracture site

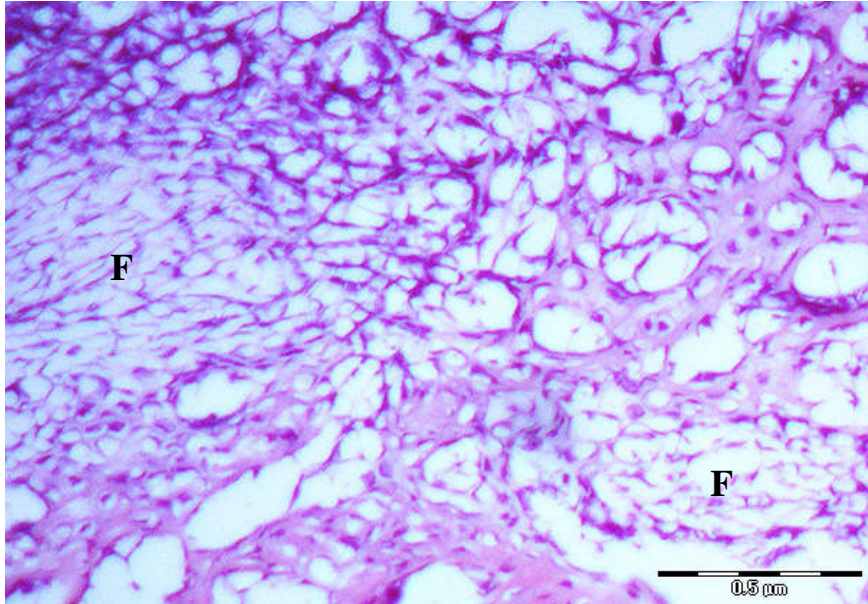


Figure 29 LIPU neurectomy group at 7 days post-fracture (H&E, 100x)
Mainly fibrous tissue (**F**) was found in the fracture site

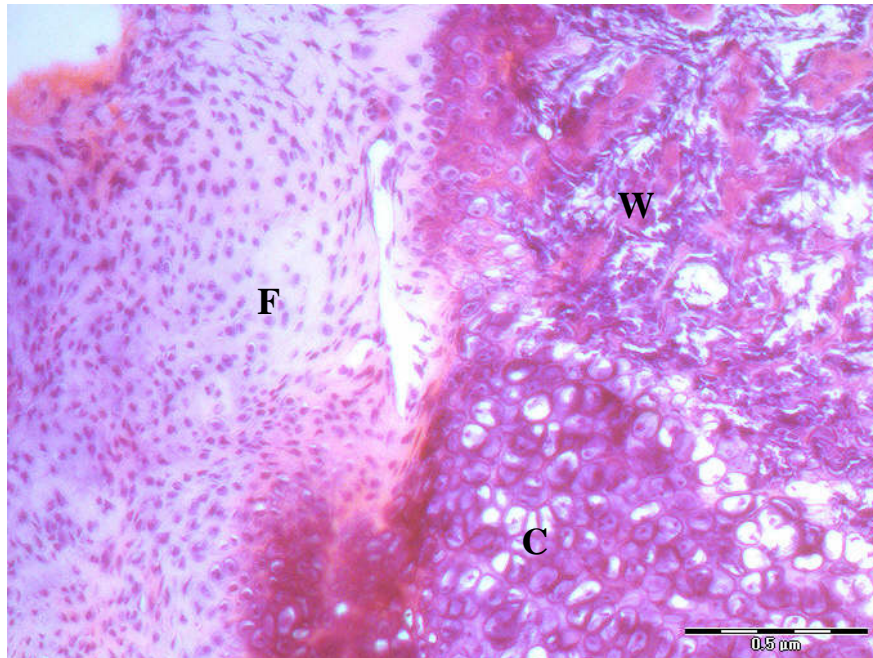


Figure 30 sham LIPU neural intact group at 14 days post-fracture (H&E, 100x)
Mixture of different types of bone tissue – fibrous (F), cartilage (C) and woven bone (W) were found in the fracture site

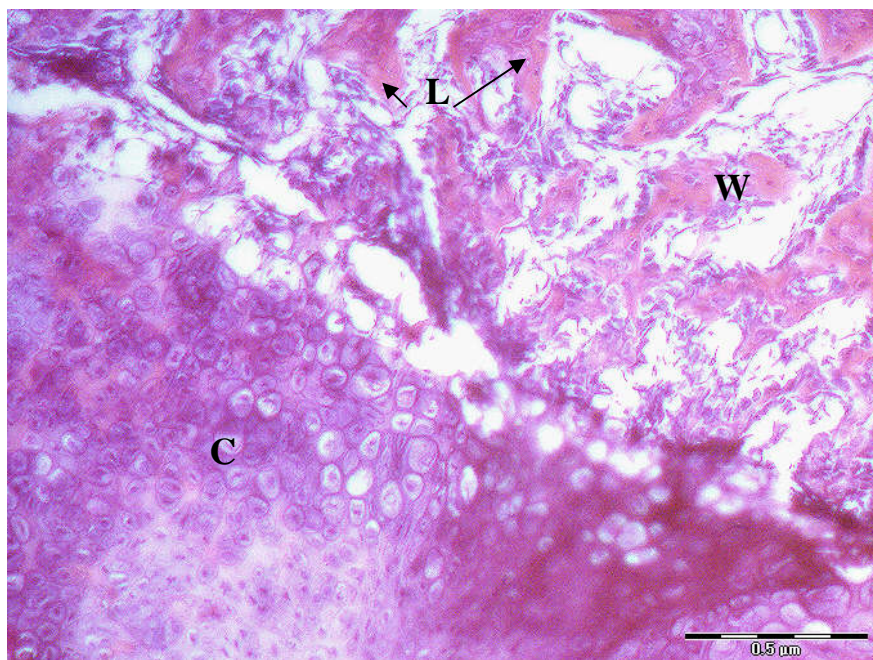


Figure 31 LIPU neural intact group at 14 days post-fracture (H&E, 100x)
Mixture of cartilage (C), woven (W) and lamella (L) bone were found in the fracture site

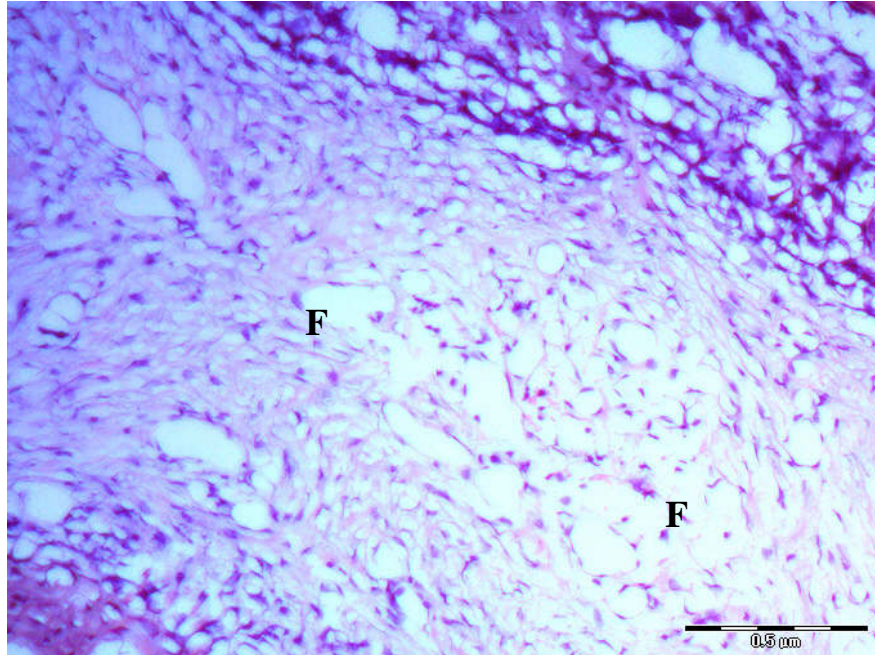


Figure 32 sham LIPU neurectomy group at 14 days post-fracture (H&E, 100x)
Fibrous tissue (**F**) was mainly found in the fracture site

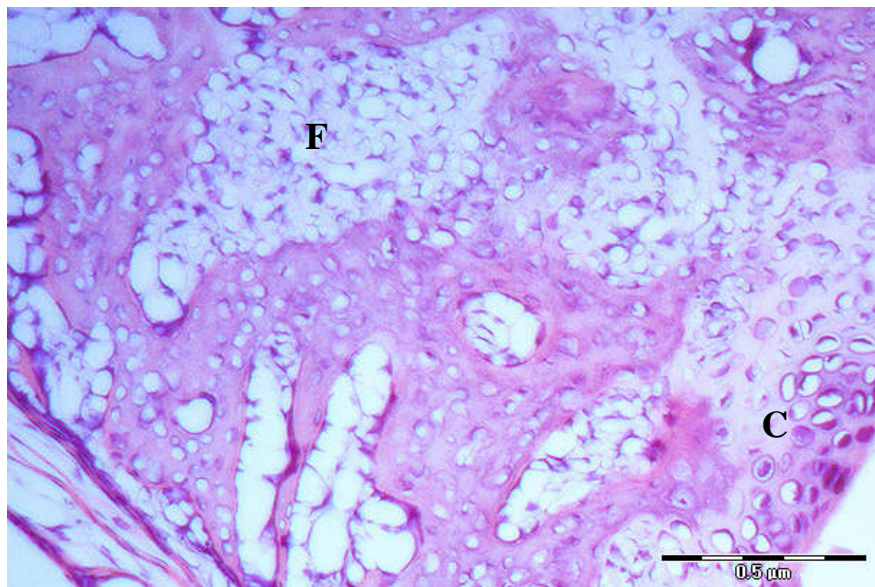


Figure 33 LIPU neurectomy group at 14 days post-fracture (H&E, 100x)
Fibrous tissue (**F**) and cartilage (**C**) were mainly found in the fracture site

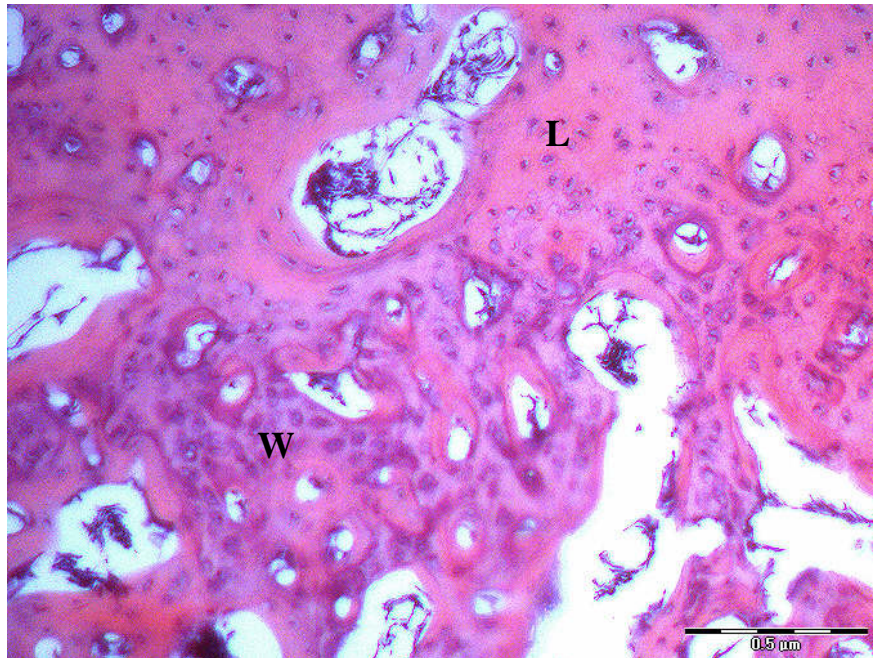


Figure 34 sham LIPU neural intact group at 21 days post-fracture (H&E, 100x)
Woven (**W**) and lamella (**L**) bone were mainly found in the fracture site

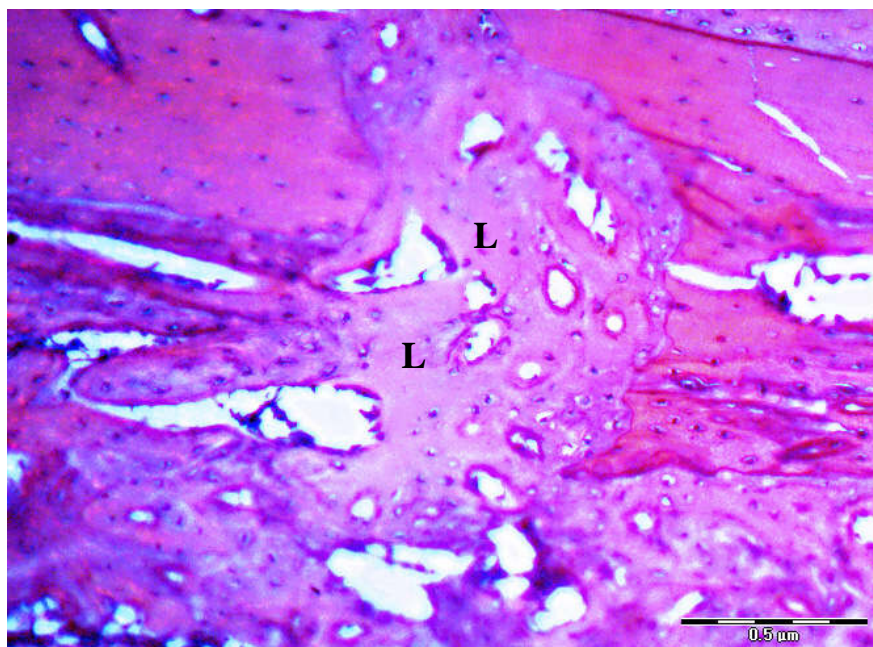


Figure 35 LIPU neural intact group at 21 days post-fracture (H&E, 100x)
Lamella bone (**L**) was mainly found in the fracture site filling the fracture gap

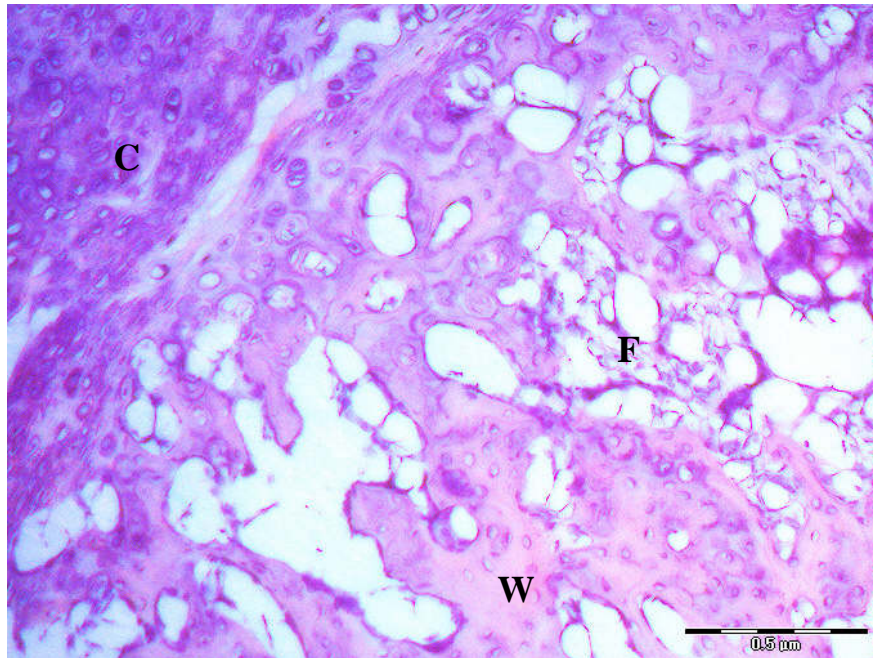


Figure 36 sham LIPU neurectomy group at 21 days post-fracture (H&E, 100x)
Mixture of fibrous tissue (F), cartilage (C) and woven (W) bone were found in the fracture site

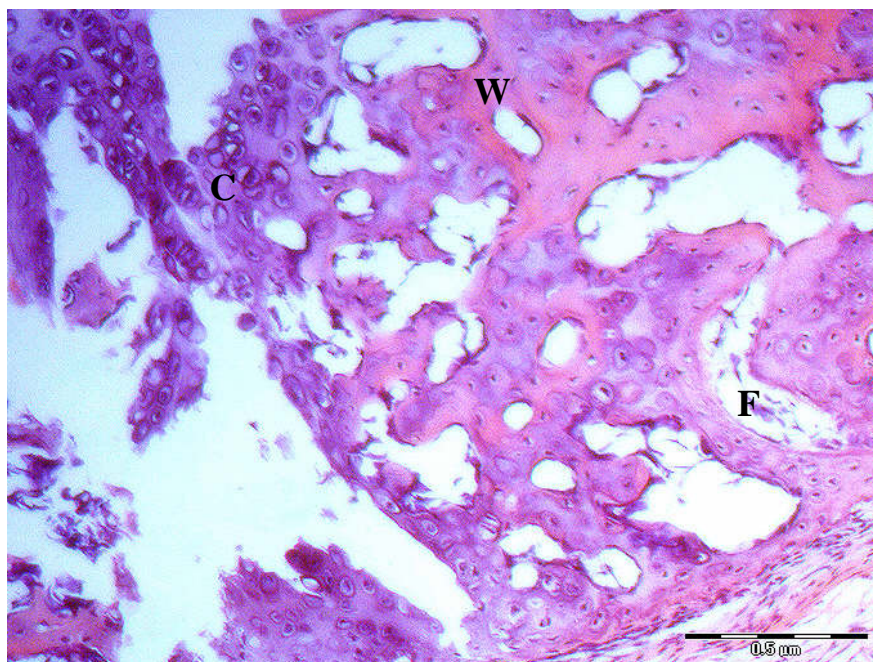


Figure 37 LIPU neurectomy group at 21 days post-fracture (H&E, 100x)
Similar to sham LIPU neurectomy group, mixture of fibrous tissue (F), cartilage (C) and woven (W) bone were found in the fracture site

Chapter 6 Discussion

6.1 Effectiveness of LIPU in enhancing fracture healing

The results of the present study reveal the effectiveness of Low Intensity Pulsed Ultrasound (LIPU) in accelerating fracture healing by developing a smaller (as indicated from the smaller callus area from pQCT measurement in the LIPU-treated group when comparing the two groups without nerve resection) yet more mature callus (as shown from the elevated union rate, bone mineral density (BMD), and findings from morphological studies between the two groups without nerve resection). This agrees with findings from previous studies that LIPU could enhance fracture healing by stimulating earlier onset and completion of callus formation, increasing the bone mineral density, and speeding up the whole ossification process and maturation of the bone (Azuma et al, 2001, Ito et al, 2000, Jinguishi et al, 1998, Takikawa et al, 2001). However, the promoting effect of LIPU on fracture healing could only be seen in those fractures with nervous supply (i.e. with intact nerves, without nerve resection). Without nervous supply as demonstrated by the sciatic nerve resection in this study, the effect of LIPU was greatly reduced or negligible as observed from the comparable union rate, bone mineral density and callus maturation from morphological studies between the two groups with neurectomy. These findings suggest the possible involvement of peripheral innervation as a mechanoreceptor in sensing and responding to mechanical stimuli generated by LIPU in fracture healing, as proposed in the present study.

6.2 Role of innervation in response to LIPU on fracture healing

As mentioned, numerous previous studies have been performed and demonstrated the important role of peripheral innervation, particularly neuropeptide-containing nerve fibers, in fracture healing (Hukkanen et al, 1993, Madsen et al, 1998, Norsletten et al, 1994, Li et al, 2001). The results of previous studies showed that in receiving nociceptive signals generated by the fracture, peripheral innervation responds by releasing certain kinds of neuropeptides, which in turn exert local effects to the site in assisting the local healing process. Several neuropeptides, like calcitonin gene related peptide (CGRP) and vasoactive intestinal peptide (VIP), have been identified. Among the neuropeptides identified, CGRP is the most frequently researched, probably because CGRP-containing sensory nerves appear to be the most abundant in bone (Hukkanen et al, 1995, Madsen et al, 1998, Zaidi et al, 1988).

CGRP is a sensory neuropeptide synthesized mainly in small and medium-sized sensory neurons in the dorsal root ganglia, and is found in small unmyelinated C and thinly myelinated A-delta fibers. It is a potent vasodilator and is believed to be associated with angiogenesis during fracture healing. Numerous *in vitro* studies demonstrate the modulatory effect of CGRP on bone metabolism by acting on osteoblasts and osteoclasts. CGRP has been shown to cause a 30- to 500-fold increase of osteoblastic cyclic adenosine monophosphate (cAMP) via acting on their specific CGRP receptors. CGRP has also been found to inhibit osteoclastic

resorption (Hukkanen et al, 1995, Madsen et al, 1998, Zaidi et al, 1988). All of these findings suggested the essential role of CGRP-containing nerve fibers in fracture healing.

Taken together, it is proposed that LIPU acts on the bone healing process through its innervation. Innervation of the bone might sense and receive these mechanical stimuli and respond to it by releasing neuropeptides, especially CGRP, into the fracture site, which in turn assists the healing process. To confirm the nervous involvement in responding to LIPU, and to test whether the neuropeptides are released as a result of the nervous response to LIPU stimulus in fracture healing, immunostaining on different types of nerve fibers as well as neuropeptides should be performed. However, due to the limited time available in this study, we were unable to perform the immunostaining to confirm this hypothesis.

6.3 Influence of nerve resection on fracture healing

Apart from demonstrating the effect of LIPU on fracture healing, the results of the present study also demonstrate the influence of nerve resection on fracture healing. Findings from the present study suggest that nerve resection results in larger, yet immature callus (as indicated from the larger callus size, lower union rate and results on morphological findings when comparing the two sham groups with and without neurectomy). These agreed with results obtained from previous work done

by others (Hukkanen et al, 1995, Madsen et al, 1998, Nordsletten et al, 1994). Several postulations have been made by previous researchers in explaining why a larger but immature callus is formed after nerve resection (Madsen et al, 1998, Nordsletten et al, 1994). Nordsletten et al (1994) proposed that motion in the fracture is recognized by innervation, which in turn initiates resorption of the bone in fractures with intact nerves. However, motion cannot be recognized and resorption of the bone cannot be initiated in a situation where sensory innervation is absent. This explains why a larger callus was formed after nerve resection. A defect in tissue composition and organization of the callus due to the lack of appropriate neural influence may explain the immaturity of the callus after nerve resection (Nordsletten et al, 1994).

6.4 Bone mineral content (BMC)

No significant main effect was found from the two factors (innervation and LIPU) on total BMC. This may be due to the fact that the total BMC was calculated from the product of the total BMD with the volume of the measured region as it could not be measured directly from the pQCT machine. The formula for calculating the total BMC is shown below.

$$\text{Total BMC (mg)} = \frac{\text{Total BMD} \times \text{Total Area} \times \text{Thickness of the slide (i.e. 1mm)}}{1000}$$

Except for the LIPU neural intact group, the results of the total BMD and those of the total area were comparable between the other three groups. It is not difficult to assume that a similar total BMC could be obtained in those three groups. Although the highest total BMD was found in the LIPU neural intact group, the lowest total area was also found in that group. The effect was cancelled out during calculation and resulted in similar total BMC in all the groups.

6.5 Ultimate load and stiffness from four-point bending test

As with total BMC, no significant main effects were found in the two factors of ultimate load and stiffness. This is probably due to the high standard deviation (nearly the same as the mean) found on both parameters among the four groups. This large standard deviation may be caused by the shear stress generated at the contact points during the test between the bone and the four-point bending jig. In the present study, a sharp jig was used. It is advised based on a previous study that a round jig be employed in bending tests in order to avoid shear stress during the test (Siu et al, 2003). Another possible explanation for this large standard deviation could be the shape and the texture of the specimens. Rats' tibiae are curved in shape and can easily slip or undergo axial rotation during the initial part of the test. This is especially true on the fracture callus tested in this experiment, where size and shape were irregular. To minimize this unwanted rotation, following Brodt et al (1999), the loading points were allowed to pivot freely so that four points of contact were

always ensured. Although this technique was used, it could not eliminate the error generated by axial rotation and which may have been the factor contributing to the large standard deviation.

In addition to the large standard deviation, the small sample size may have contributed to the non-significant findings. As mentioned, some of the tibiae broke during pin removal, and mechanical data could not be obtained from these tibiae. The broken tibiae were regarded as nonunion. Although statistically significant difference could not be obtained in the mechanical test, by counting the ratio of the numbers of broken tibiae to those that did not (union rate) and combining this with the mechanical test results, we could also identify which group was superior.

Comparing the mechanical testing results from the present study with those obtained from a similar study performed by Bak & Andreassen (1988), although three-point instead of four-point bending was used in the previous study, it is observed that the findings from the intact tibiae were comparable (ultimate load: 149.72 ± 9.8 N in the present study and 112 ± 8 N in Bak & Andreassen; stiffness: 304.23 ± 25.02 N/mm in the present study and 307 ± 33 N/mm in Bak & Andreassen). However, when comparing results between the fractured limbs, our findings were that the limbs were about 3 (from 2.9 to 4.6 times) times stronger than those in the previous study (ultimate load: 46.42 ± 34.77 N in the present study and 16 ± 2 N in Bak & Andreassen; stiffness: 147.27 ± 129.78 N/mm in the present study and 31.9 ± 7.3 N/mm in Bak & Andreassen). Similar results as well as a small standard deviation

on intact tibiae between the present and previous study suggest the validity of the mechanical testing device. The great differences in the results obtained from the fractured limbs between the two studies may be due to the fact that the fractures were of different levels in the two studies. In the present study, fractures were created on the mid shaft of the tibia, while in the previous study performed by Bak & Andreassen (1988), fractures were created at 2mm about the tibio-fibular junction. As suggested by Bak & Jensen, (1992), there was a great difference in the mechanical strength between fractures at different levels in the bone shaft.

In another study done by An et al (1994), where the fracture was created at the same level as in the present study, ultimate load and stiffness on the fracture tibiae were 72 ± 29 N and 121 ± 73 N/mm respectively. The differences between the study performed by An et al and our study may have resulted from the different testing methods (three-point bending in the previous study vs. four-point bending in the present study). Due to practical problems in clamping and aligning the bone on the testing machine, a bending test instead of a torsional test was performed in this study. It is generally assumed that in four-point bending, the bone will be fractured at the weakest point, while in three point bending, the bone will be fractured at the point where the force is applied (fracture line) (Bak & Jensen, 1992). In the present study, the bone was carefully monitored during the whole testing process and it was found that all the tibiae broke at the fracture line during the test. Therefore, the results obtained from present study should be the same as those obtained by using three-point bending. This is confirmed by the results obtained from intact bone,

where the results from this study (using four-point bending) are comparable with those of a previous study (using three-point bending) as mentioned above. To explain the differences between these two studies (An et al, 1994 and the present study), it is proposed that the mechanical testing device used in the present study may not be suitable for testing irregularly shaped bone (as can be seen from the great standard deviation on fractured limbs in the present study). Further modifications of the testing device, e.g. using a round head testing jig, are suggested.

6.6 Mechanical test findings from previous studies on LIPU

According to Wang et al (1994), using the same signal parameters of LIPU as in the present study on rat femora, it was found that the maximum torque to failure was on average 22% greater and the stiffness 67% (i.e. significantly) greater than that of the contralateral, control femora. However, in the present study, the ultimate load and stiffness (from four-point bending on the tibiae) were 27% and 22% lower than in the control group (compared between the LIPU neural intact group and sham LIPU neural intact group). Although this difference might have been caused by the difference in testing method and difference in the tested limb, it may have been largely caused by the error generated by the mechanical test as mentioned.

6.7 Mechanical test findings from previous studies on nerve resection

In the present study, the tibiae regained 29% of the ultimate load and 34% of the stiffness after nerve resection (i.e. sham LIPU neurectomy). After the sham operation (i.e. sham LIPU neural intact), the tibiae regained 27% of the ultimate load and 43% of the stiffness. This differs from the findings of previous researchers, where 7% to 11% of the mechanical strength (from torsional testing) was regained in the nerve-resected and sham operated group (no nerve resection) in the study by Nordsletten et al (1994), and in another study performed by Madsen et al (1998), 20% and 50% of the mechanical strength (from torsional testing) was regained in the nerve-resected and sham-operated group (no nerve resection). Again, although these differences could also be due to the difference in testing methods, they may largely be generated by error during the mechanical test.

6.8 Correlations on bone strength

It has been recommended that the mechanical test is the gold standard in evaluating bone healing (Blokhuis et al, 2000). Numerous studies have been performed looking at the relationship between the data obtained from the pQCT machine and the mechanical strength of bone. It has been found that the bone mineral density (BMD), bone mineral content (BMC) and stress strain index (SSI) measured from pQCT are able to predict the intact bone strength in animal models and can be used in

predicting fracture risk in osteoporosis (Augat et al, 1997, Giavaresi et al, 1999, Siu et al, 2003, Volkman et al, 2004). Recently, several studies have been conducted using pQCT to monitor the healing process. Previous studies have proposed the use of pQCT to provide a non-invasive and objective tool for quantifying bone strength in healing callus. Augat et al (1997), using a sheep tibial osteotomy model, suggested that there was a strong correlation between the volumetric BMD of the osteotomy gap with the biomechanical findings ($R^2=0.70$) after 9 weeks of healing time. However, there was no or even negative correlations between the parameters measured by pQCT and the biomechanical findings in the present study. There are several factors contributing to this. Giavaresi et al (1999) suggested that the mechanical properties of a bone depend on two main factors, the composition (the porosity, the mineralization and the density) and the organization (the trabecular and cortical bone architecture) of bone materials. In the study done by Augat et al (1997), mechanical properties and pQCT were measured in sheep at 9 weeks post-fracture, where the fractured callus was healed and remodeled. However, in the present study, mechanical properties and pQCT were measured at only 3 weeks post-fracture. According to An et al (1994), tibiae were regarded as healed in rats at 5 weeks post-fracture. Therefore, in the present study, the fractured callus was not completely healed and remodeled, which means that the minerals and collagen were not well organized in the callus. Even if there is a high mineral density in the callus, without good organization, the bone strength could still be low. This could explain why the parameters measured from pQCT did not correlate with the mechanical strength of the bone. Another reason for this is probably the fact that in the previous

study, only newly formed bone was detected, while in the present study, due to the impracticality of isolating the newly formed bone by machine (no such option), all bone materials (including the old bone) in the callus were measured. In the present study, data from pQCT were obtained after averaging results from 3 slides (mean value of each parameter within the callus), while the mechanical properties (ultimate load and stiffness) were measured at a point in the four-point bending test. This may be another reason why the two measurements did not correlate. The large standard deviation obtained from mechanical testing may also contribute to the uncorrelated findings between the pQCT and mechanical strength.

6.9 Correlations on callus size

Although significant correlation was found between the callus index evaluated by X ray and the callus area measured by pQCT, there was only a fair degree of relationship. This fair degree of relationship could be due to the differences in the types of measurement used. In measuring the callus index by X ray, the image of the tibia was a projectional image and the diameter of the bone depended on the position of the tibia, whereas in measuring the callus size using pQCT, it was measured from a 3-dimensional image regardless of the position of the tibia during measurement. Another reason for the fair degree of relationship was that the callus index was measured on a single line while the callus area, similar to the bone

mineral density and bone mineral content, was obtained after averaging the results from 3 slides (i.e. the mean area of the whole callus).

6.10 Histological findings

When comparing the histological findings from the present study (sham LIPU control group) with those of a previous study performed by Einhorn (1998), who studied the morphological changes after fracture healing in rats, our results coincide with the earlier findings. Both of the studies demonstrated that on day 7 after fracture, fibrous tissue was mainly found in the callus region. By day 14 post-fracture, abundant amounts of chondroid tissue were seen, and woven bone was seen on day 21 after fracture.

6.11 Limitations

There were a few limitations to this study. For the decalcified sections, in order to obtain a more objective result, quantitative analysis (i.e. total callus area, area of different types of tissues and amount of different types of cells) rather than subjective qualitative analysis (used in the present study) should be carried out. Also, different types of staining specific for different types of bone, like Safranin O for

staining cartilage, should be performed. However, due to the limited time in the present study, only qualitative analysis and H&E staining were performed.

As mentioned, the tibiae of the rats in this study were regarded as healed after 5 weeks post-fracture. Rats should be kept for a longer period before being euthanized in the future.

Chapter 7 Conclusions

As with previous studies, the results of present study confirm the accelerating effect of LIPU on fracture healing as indicated by elevated union rate, bone mineral density and maturation rate of callus after LIPU treatment.

Moreover, the results of present study also demonstrate the important role of peripheral innervation in the healing process as suggested by the reduced union and maturation rate after nerve resection.

The current study is the first study to investigate the relationship between LIPU and sensory innervation in bone in fracture healing. The findings from this study address the importance of callus innervation in sensing and responding to mechanical stimuli generated by LIPU in fracture healing, as proposed in the present study. It is hoped that the current work will stimulate further research. More studies are required to examine the relationship between LIPU and sensory innervation in bone and how they interact with each others in fracture healing.

References

1. Adams, J.C. (1999). *Outline of fractures, including joint injuries 11th ed.* Edinburgh, New York. Churchill Livingstone.
2. American Academy of Orthopaedic Surgeons. (2002). Retrieved from <http://www.aaos.org/>
3. An, Y.H., Friedman, T.P., & Robert, A.D. (1994). Production of a standard closed fracture in the rat tibia. *Journal of Orthopaedic Trauma*, 8:111-115.
4. Aro, H. (2001). Development of nonunions in the rat fibula after removal of periosteal neural mechanoreceptors. *Clinical Orthopaedics and Related Research*, 199:292-299.
5. Aro, H., Eerola, E., Aho, A.J., & Penttinen, R. (1981). Healing of experimental fractures in the denervated limbs of the rat. *Clinical Orthopaedics and Related Research*, 155: 211-217.
6. Augat, P., Merk, J., Genant, H.K., & Claes, L. (1997). Quantitative assessment of experimental fracture repair by peripheral computed tomography. *Calcified Tissue International*, 60: 194-199.
7. Augat, P., & Ryaby J.T. (2001). Fracture healing and micro architecture. *Advances in Experimental Medicine and Biology*, 469: 99-110.
8. Azuma, Y., Ito, M., Harada, Y., Takagi, H., Ohta, T., & Jingushi, S. (2001). Low-intensity pulsed ultrasound accelerates rat femoral fracture healing by acting on the carious cellular reactions in the fracture callus. *Journal of Bone and Mineral Research*, 16: 671-680.
9. Bak, B., & Andreassen, T.T. (1988). Reduced energy absorption of healed fracture in the rat. *Acta Orthopaedica Scandinavica*, 59: 548-551.
10. Bak, B., & Jensen, K.S. (1992). Standardization of tibial fractures in the rat. *Bone*, 13: 289-295.
11. Blokhuis, T.J., den Boer, F.C., Bramer, J.A., van Lingen, A., Roos, J.C., Bakker, F.C., Patka, P., & Haarman, H.J. (2000). Evaluation of strength of healing fractures with dual energy X ray absorptiometry. *Clinical Orthopaedics and Related Research*, 380: 260-268.
12. Bonnarens, F., & Einhorn, T.A. (1984). Production of a standard closed fracture in laboratory animal bone. *Journal of Orthopaedic Research*, 2: 97-101.

13. Brodt, M.D., Ellis, C.B., & Silva, M.J. (1999). Growing C57B1/6 mice increase whole bone mechanical properties by increasing geometric and material properties. *Journal of Bone and Mineral Research*, 14: 2159-2166.
14. Cheng, J.C., Qin, L., Cheung, C.S., Sher, A.H., Lee, K.M., Ng, S.W., & Guo, X. (2000). Generalized low areal and volumetric bone mineral density in adolescent idiopathic scoliosis. *Journal of Bone and Mineral Research*, 15: 1587-1595.
15. Cornell, C.N., & Lane, J.M. (1992). Newest factors in fracture healing. *Clinical Orthopaedics and Related Research*, 277: 297-311.
16. Corradi, C., & Cozzolino, A. (2001). Ultrasound and bone callus formation during function. *Acta Orthopaedica Scandinavica*, 66: 77-98.
17. Duarte, L.R. (1983). The stimulation of bone growth by ultrasound. *Archives of Orthopaedic and Traumatic Surgery*, 101: 153-159.
18. Dyck, P.J., Stevens, J.C., O'Brien, P.C., Oviatt, K.F., Lais, A.C., Coventry, M.B., & Beabout, J.W. (1983). Neurogenic arthropathy and recurring fractures with subclinical inherited neuropathy. *Neurology*, 33: 357-367.
19. Einhorn, T.A. (1995). Enhancement of fracture-healing. *Journal of Bone and Joint Surgery – American Volume*, 77: 940-956.
20. Einhorn, T.A. (1998). The cell and molecular biology of fracture healing. *Clinical Orthopaedics and Related Research*, 355 Supp: 7-21.
21. El-Mowafi, H., & Mohsen, M. (2005). The effect of low-intensity pulsed ultrasound on callus maturation in tibial distraction osteogenesis. *International Orthopaedics*, 29: 121-124.
22. Fujioka, H., Tsunoda, M., Noda, M., Matsui, N., & Mizuno, K. (2000). Treatment of ununited fracture of the hook of hamate by low-intensity pulsed ultrasound: a case report. *Journal of Hand Surgery – American volume*, 25: 77-79.
23. Fyfe, M.C., & Chahl, L.A. (1982). Mast cell degranulation: a possible mechanism of action of therapeutic ultrasound. *Ultrasound in Medicine and Biology*, 8 Supp: 62.
24. Fyfe, M.C., & Chahl, L.A. (1985). The effect of single or repeated applications of "therapeutic" ultrasound on plasma extravasation during silver nitrate induced inflammation of the rat hindpaw ankle joint in vivo. *Ultrasound in Medicine and Biology*, 11: 273-283.

25. Garcia-Castellano, J.M., Diaz-Herrera, P., & Morcuende, J.A. (2000). Is bone a target-tissue for the nervous system? New advances on the understanding of their interactions. *Iowa Orthopaedic Journal*, 20: 49-58.
26. Gebauer, G.P., Lin, S.S., Beam, H.A., Vieira, P., & Parsons, J.R. (2002). Low intensity pulsed ultrasound increases the fracture callus strength in diabetic BB Wistar rats but does not affect cellular proliferation. *Journal of Orthopaedic Research*, 20: 587-592.
27. Giavaresi, G., Fini, M., Gnudi, S., Mongiorgi, R., Ripamonti, C., Zati, A., & Giardino, R. (1999). The mechanical properties of fluoride treated bone in the ovariectomized rat. *Calcified Tissue International*, 65: 237-241.
28. Greenbaum, M.A., & Kanat, I.O. (1993). Current concepts in bone healing. Review of the literature. *Journal of the American Podiatric Medical Association*, 83: 123-129.
29. Guo, X. (1994). Histomorphological study of Interface between Shanz screw and cortical bone in a sheep tibia fracture model. (MD Thesis)
30. Hadjiargyrou, M., McLeod, K., Ryaby, J.P., & Rubin, C. (1998). Enhancement of fracture healing by low intensity ultrasound. *Clinical Orthopaedics and Related Research*, 355 Supp: 216-229.
31. Heckman, J.D., Ryaby, J.P., McCabe, J., Frey, J.J., & Kilcoyne, R.F. (1994). Acceleration of tibial fracture-healing by non-invasive, low-intensity pulsed ultrasound. *Journal of Bone and Joint Surgery - American Volume*, 76: 26-34.
32. Hukkanen, M., Konttinen, Y.T., Santavirta, S., Nordsletten, L., Madsen, J.E., Almaas, R., Oestreicher, A.B., Rootwelt, T., & Polak, J.M. (1995). Effect of sciatic nerve section on neural ingrowth into the rat tibial fracture callus. *Clinical Orthopaedics and Related Research*, 311: 247-257.
33. Hukkanen, M., Konttinen, Y.T., Santavirta, S., Paavolainen, P., Gu, X.H., Terenghi, G., & Polak, J.M. (1993). Rapid proliferation of calcitonin gene-related peptide-immunoreactive nerves during healing of rat tibial fracture suggests neural involvement in bone growth and remodeling. *Neuroscience*, 54: 969-979.
34. Ito, M., Azuma, Y., Ohta, T., & Komoriya, K. (2000). Effects of ultrasound and 1,25-dihydroxyvitamin D3 on growth factor secretion in co-cultures of osteoblasts and endothelial cells. *Ultrasound in Medicine and Biology*, 26: 161-166.

35. Jamsa, T., Koivukangas, A., Kippo, K., Hannuniemi, R., Jalovaara, P., & Tuukkanen, J. (2000). Comparison of radiographic and pQCT analyses of healing rat tibial fractures. *Calcified Tissue International*, 66: 288-291.
36. Jingushi, S., Azuma, Y., Ito, M., Harada, Y., Takagi, H., Ohta, T., & Komoriya, K. (1998). Effects of non invasive pulsed ultrasound on rat femoral fracture. *Third World Congress of Biomechanics*, 175b.
37. Jingushi, S., Joyce, M.E., & Bolander, M.E. (1992). Genetic expression of extracellular matrix proteins correlates with histologic changes during fracture repair. *Journal of Bone and Mineral Research*, 7: 1045-1055.
38. Kimmel, D.B., Moran, E.L., & Bogoch, E.R. (1999). Animal methods of osteopenia or osterporosis. In An, Y.H., & Friedman, R.J. (1999). *Animal Models in Orthopaedic Research. USA. CRC Press LLC*.
39. Klineberg, I., & Murray, G. (1999). Osseoperception: sensory function and proprioception. *Advances in Dental Research*, 13: 120-129.
40. Konttinen, Y., Imai, S., & Suda, A. (1996). Neuropeptides and the puzzle of bone remodeling. State of the art. *Acta Orthopaedica Scandinavica*, 67: 632-639.
41. Kristiansen, T.K., Ryaby, J.P., McCabe, J., Frey, J.J., & Roe, L.R. (1997). Accelerated healing of distal radial fractures with the use of specific, low-intensity ultrasound. A multicenter, prospective, randomized, double-blind, placebo-controlled study. *Journal of Bone and Joint Surgery - American Volume*, 79: 961-973.
42. Kuntz, A., & Richins, C.A. (1945). Innervation of the bone marrow. *Journal of Comparative Neurology*, 83: 213-222.
43. LaStayo, P.C., Winters, K.M., & Hardy, M. (2003). Fracture healing: bone healing, fracture management, and current concepts related to the hand. *Journal of Hand Therapy*, 16: 81-93
44. Leung, K.S., Cheung, W.H., Zhang, C., Lee, K.M. & Lo, H.K. (2004). Low intensity pulsed ultrasound stimulates osteogenic activity of human periosteal cells. *Clinical Orthopaedics and Related Research*, 418: 253-259.
45. Leung, K.S., Lee, W.S., Tsui, H.F., Liu, P.P.L. & Cheung, W.H. (2003). Complex tibial fracture outcomes following treatment with low-intensity pulsed ultrasound. *Ultrasound in Medicine and Biology*, 30: 389-395.

46. Leung, K.S., Siu, W.S., Cheung, N.M., Lui, P.Y., Chow, D.H., James, A., & Qin, L. (2001). Goats as osteopenic animal model. *Journal of Bone and Mineral Research*, 16: 2348-2355.
47. Li, J., Ahmad, T., Spetea, M., Ahmed, M., & Kreicbergs, A. (2001). Bone reinnervation after fracture: a study in the rat. *Journal of Bone and Mineral Research*, 16: 1505-1510.
48. Lind, M. (1996). Growth factors: possible new clinical tools. A review. *Acta Orthopaedica Scandinavica*, 67: 407-417.
49. Madsen, J.E., Hukkanen, M., Aspenberg, P., Polak, J., & Nordsletten L. (2000). Time-dependent sensory nerve ingrowth into a bone conduction chamber. *Acta Orthopaedica Scandinavica*, 71: 74-79.
50. Madsen, J.E., Hukkanen, M., Kristian, A.A., Basran, I., Moller, J.F., Polak, J.M., & Nordsletten, L. (1998). Fracture healing and callus innervation after peripheral nerve resection in rats. *Clinical Orthopaedics and Related Research*, 351: 230-240.
51. Martin, F.H., (2004). *Fundamentals of Anatomy & Physiology 6th ed.* N.J. Prentice Hall.
52. Mayr, E., Frankel, V., & Ruter, A. (2000). Ultrasound – an alternative healing method for nonunions? *Archives of Orthopaedic and Trauma Surgery*, 120: 1-8.
53. National Osteoporosis Foundation. (2002). Retrieved from <http://www.nof.org/osteoporosis/stats.htm>.
54. Nolte, P.A., van der Krans, A., Patka, P., Janssen, I.M.C., Ryaby, J.P. & Albers, G.H.R. (2001). Low intensity pulsed ultrasound in the treatment of nonunions. *Journal of Trauma Injury Infection and Critical Care*, 51: 693-702.
55. Nordsletten L., Madsen J. E., Almaas, R., Rootwelt T., Halse, J., Konttinen, Y.T., Hukkanen, M., & Santavirta, S. (1994). The neuronal regulation of fracture healing. Effects of sciatic nerve resection in rat tibia. *Acta Orthopaedica Scandinavica*, 65: 299-304.
56. Onuoha, G.N. (2001). Circulating sensory peptide levels within 24h or human bone fracture. *Peptides*, 22: 1107-1110.
57. Onuoha, G.N., & Alpar, E.K. (2000). Elevation of plasma CGRP and SP levels in orthopedic patients with fracture neck of femur. *Neuropeptides*, 34: 116-120.

58. Ozaki, A., Tsunoda, M., Kinoshita, S., Saura, R. (2000). Role of fracture hematoma and periosteum during fracture healing in rats: interaction of fracture hematoma and the periosteum in the initial step of the healing process. *Journal of Orthopaedic Science*, 5: 64-70.
59. Parvizi, J., Parpura, V., Kinnick, R.R., Greenleaf, J.F. (1997). Low intensity ultrasound increases intracellular concentration of calcium in chondrocytes. *TransAmerican Orthopaedic Research Society*, 22: 465.
60. Parvizi, J., Wu, C.C., Lewallen, D.G., & Greenleaf, J.F., & Bolander, M.E. (1999). Low-intensity ultrasound stimulates proteoglycan synthesis in rat chondrocytes by increasing aggrecan gene expression. *Journal of Orthopaedic Research*, 17: 488-494.
61. Pilla, A.A., Mont, M.A., Nasser, P.R., Khan, S.A., Figueiredo, M., Kaufman, J.J., & Siffert, R.S. (1990). Non-invasive low-intensity pulsed ultrasound accelerates bone healing in the rabbit. *Journal of Orthopaedic Trauma*. 4: 246-253.
62. Portney LG, Watkins MP. (2000). *Foundations of clinical research: applications to practice 2nd ed.* N.J. Prentice Hall Health.
63. Qin, L., Chan, K.M., Rahn, B., & Guo, X. (1997). Bone mineral content measurement using pQCT for predicting the cortical and trabecular bone mechanical properties. *Chinese Journal of Orthopaedics*, 17: 66-70.
64. Rawool, N.M., Goldberg, B.B., Forsberg, F., Winder, A.A., Tallah, R.J., & Hume, E. (2003). Power doppler assessment of vascular changes during fracture treatment with low intensity ultrasound. *Journal of Ultrasound in Medicine*, 22: 145-153.
65. Remedios, A., (1999). Bone and bone healing. *Fracture Management and Bone Healing*, 29: 1029-1044.
66. Rubin, C., Bolander, M., Ryaby, J.P., & Hadjiargyrou, M. (2001). The use of low intensity ultrasound to accelerate the healing of fractures. *Journal of Bone and Joint Surgery - American Volume*, 83: 259-270.
67. Ryaby, J.T., Bachner, E.J., Bendo, J.A., Dalton, P.F., Tannenbaum, S., & Pilla, A.A. (1989). Low intensity pulsed ultrasound increases calcium incorporation in both differentiating cartilage and bone cell cultures. *TransAmerican Orthopaedic Research Society*, 14: 15.
68. Ryaby, J.T., Mathew, J., & Duarte-Alves, P. (1992). Low intensity pulsed ultrasound affects adenylate cyclase and TGF- β synthesis in osteoblastic cells. *TransAmerican Orthopaedic Research Society*, 17: 590.

69. Sarisozen, B., Durak, K., Dincer, G., Bilgen O.F. (2002). The effects of vitamins E and C on fracture healing in rats. *The Journal of International Medical Research*, 30: 309-313.
70. Simmons, D.J. (1985). Fracture healing perspectives. *Clinical Orthopaedics and Related Research*, 200: 100-113.
71. Siu, W.S., Qin, L., & Leung, K.S. (2003). pQCT bone strength index may serve as a better predictor than bone mineral density for long bone breaking strength. *Bone and Mineral Metabolism*, 21: 316-322.
72. Takikawa, S., Matsui, N., Kokubu, T., Tsunoda, M., Fujioka, H., Mizuno, K., & Azuma, Y. (2001) Low-intensity pulsed ultrasound initiates bone healing in rat nonunion fracture model. *Journal of Ultrasound in Medicine*, 20: 197-205.
73. Tanzer, M., Harvey, E., Kay, A., Morton, P., & Bobyn, J.D. (1996). Effect of noninvasive low intensity ultrasound on bone growth into porous-coated implants. *Journal of Orthopaedic Research*, 14: 901-906.
74. Thurston, T.J. (1982). Distribution of nerves in long bones as shown by silver impregnation. *Journal of Anatomy*, 134: 719-728.
75. Utvag, S.E., Grundnes, O., & Reikeras, O. (1998). Graded exchange reaming and nailing of non-unions. Strength and mineralization in rat femoral bone. *Archives of Orthopaedic and Trauma Surgery*. 118: 1-6.
76. Utvag, S.E., & Reikeras, O. (1998). Effects of nail rigidity on fracture healing. Strength and mineralization in rat femoral bone. *Archives of Orthopaedic and Trauma Surgery*, 118: 7-13.
77. van Steenberghe, D. (2000). From osseointegration to osseoperception. *Journal of Dental Research*, 79: 1833-1837.
78. Volkman, S.K., Galecki, A.T., Burke, D.T., Miller, R.A., & Goldstein, S.A. (2004). Quantitative trait loci that modulate femoral mechanical properties in a genetically heterogeneous mouse population. *Journal of Bone and Mineral Research*, 19: 1497-1505.
79. Wang, S.J., Lewallen, D.G., Bolander, M.E., Chao, E.Y., Ilstrup, D., & Greenleaf, J.F. (1994). Low intensity ultrasound treatment increases strength in a rat femoral fracture model. *Journal of Orthopaedic Research*, 12: 40-47.

80. Warden, S.J., Bennell, K.L., McMeeken, J.M., & Wark, J.D. (2000). Acceleration of fresh fracture repair using the sonic accelerated fracture healing system (SAFHS): A review. *Calcified Tissue International*, 66: 157-163.
81. Warden, S.J., Favalaro, J.M., Bennell, K.L., McMeeken, J.M., Ng, K.W., Zajac, J.D., & Wark, J.D. (2001). Low-intensity pulsed ultrasound stimulates a bone-forming response in umr-106 cells. *Biochemical and Biophysical Research Communications*, 286: 443-450.
82. Wu, C.C., Lewallen, D.G., Bolander, M.E., Bronk, J., Kinnick, R., & Greenleaf, J.F. (1996). Exposure to low intensity ultrasound stimulates aggrecan gene expression by cultured chondrocytes. *TransAmerican Orthopaedic Research Society*, 22: 622.
83. Yang, K.H., & Park, S.J. (2001). Stimulation of fracture healing in a canine ulna full-defect model by low-intensity pulsed ultrasound. *Yonsei Medical Journal*, 42: 503-508.
84. Yang, K.H., Parvizi, J., Wang, S.J., Lewallen, D.G., Kinnick, R.R., Greenleaf, J.F., & Bolander, M.E. (1996). Exposure to low intensity ultrasound increases aggrecan gene expression in a rat femur fracture model. *Journal of Orthopaedic Research*, 14: 802-809.
85. Young, B., & Heath, J.W. (2000). *Functional Histology: a text and colour atlas 4th ed.* Edinburgh, New York. Churchill Livingstone.
86. Ysander, M., Branemark, R., Olmarker, K., & Myers, R.R. (2001) Intramedullary osseointegration: development of a rodent model and study of histology and neuropeptide changes around titanium implants. *Journal of Rehabilitation Research & Development*, 38: 183-190.
87. Zaidi, M., Chambers, T.J., Bevis, P.J., Beacham, J.L., Gaines Das, R.E., & MacIntyre, I. (1988). Effects of peptides from the calcitonin genes on bones and bone cells. *Quarterly Journal of Experimental Physiology*, 73: 471-485.

Appendix I: Ethical Approval issued by the Ethics Committee of the Hong Kong Polytechnic University



THE HONG KONG
POLYTECHNIC UNIVERSITY
香港理工大學

MEMO

To : Dr Guo Xia, Department of Rehabilitation Sciences
From : Dr Maureen Boost, Chairman, Animal Subjects Ethics Sub-committee
Ref. : _____ Your Ref. : _____
Tel. No. : Ext. 6391 Date : _____

Ethical approval granted for teaching / research projects using animals
[Effect of acoustic pressure waves on callus innervation and fracture healing]
(ASESC No. 01/12)

I am pleased to inform you that approval has been given to extend the approval validity period for the above project up to 13 December 2005. You will be invited to advise on the status of your project by the end of the approval validity period.

You are required to inform the Animal Subjects Ethics Sub-committee if at any time the conditions under which the animals are kept and cared for no longer fully meet the requirements of the Procedures for the Care of Laboratory Animals. If you are keeping animals in the University's animal holding room, you should state the full title of the approved project and the ASESC no. on the cage cards of the cages holding the animals. The members of the Sub-committee may visit the animal holding room unannounced at any reasonable time.

I would like to draw your attention to the University requirement that holders of licences under Cap. 340 must provide the Animal Subjects Ethics Sub-committee with a copy of their licences and a copy of their annual returns to the Licensing Authority. These must be kept up to date for the duration of the above work. In this connection, you are requested to provide to Sub-committee with the updated license for the project when available.

Dr Maureen Boost
Chairman
Animal Subjects Ethics Sub-committee

c.c. Chairman, DRC (RS)

Appendix II: License to Conduct Experiments

衛生署
九龍區辦事處
九龍亞答街 147B 號
醫院管理局大樓 一字樓



DEPARTMENT OF HEALTH
REGIONAL OFFICE (KOWLOON)
1st FLOOR,
HOSPITAL AUTHORITY BUILDING
147B ARGYLE STREET
KOWLOON

本署檔號 Our Ref.: (30) in DH/KRO/P07/01/2

19 May 2003

電話 Tel.: 2199 9100

傳真 Fax: 2311 7537 (General Office)
2375 6451 (Health Office)

Ms. LAM Wai-ling
Rehabilitation Science
The Hong Kong Polytechnic University
Hung Hom
Kowloon

Dear Madam,

**Animals (Control of Experiments) Ordinance
Chapter 340**

I refer to your letter dated 11.4.2003 and forward herewith the following licence and teaching permit issued under the captioned Ordinance :-

Form 2 : Licence to Conduct Experiments

Your attention is drawn to regulations 4 and 5 of the Animals (Control of Experiments) Regulations, copy of these regulations together with copies of Forms 6 and 7 are enclosed for your convenience. Failure to comply with either regulation 4 or regulation 5 is an offence, each offence punishable by a fine of HK\$500 and to imprisonment for 3 months. Conviction of an offence against either regulation 4 or regulation 5 or failure to comply with either regulation may result in your licence being cancelled.

Please also be reminded that if you wish to continue your experiments after the specified periods as stated on the above licence, you should renew them at least one-month before the end-dates. On the other hand, if you have completed or stopped your experiments before the specified periods, you should inform this Office immediately.

Yours faithfully,

(Ms. Sharon HOON)
for Community Physician (Kowloon)
Department of Health

SP/yl
(Licensing)

We are committed to providing quality client-oriented service

Form 2

Licence to Conduct Experiments

Name : Ms. LAM Wai-ling
Address : Rehabilitation Science,
The Hong Kong Polytechnic University

By virtue of section 7 of the Animals (Control of Experiments) Ordinance, Chapter 340, the above-named is hereby licensed to conduct the type of experiment(s), at the place(s) and upon the conditions, hereinafter mentioned.

Type of experiment(s)

The aim of the experiment is to study the effectiveness of ultrasound therapy in bone fracture healing. Fracture of femur will be induced for the rats under anaesthesia. Sciatic nerve will be resected for the nerve resection group. Different modalities of ultrasound will be applied daily according to different groups. At the end of the experiment, animals will be sacrificed by overdose of anaesthesia. The femur harvested will be used for histological and biochemical analysis.

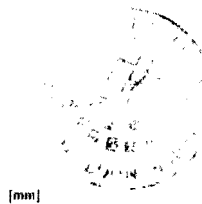
Place(s) where experiment(s) may be conducted

The Hong Kong Polytechnic University

Conditions

1. Such experiments may be conducted only for research investigation.
2. The validity of this licence is from 13.5.2003 to 12.5.2005.

Dated 13 May, 2003



[mm]

(Dr. S.Y. LEE)
for Director of Health
Licensing Authority

Appendix III: Conference Abstracts

1. Guo X, **Lam WL**, Kwong SC, Leung KS (2003): Effect of peripheral nerve injury on callus formation and fracture healing. *The 23rd Hong Kong Orthopedic Association Annual Congress, November 8-9, Hong Kong.*
2. Guo X, Liu Mu Qing, **Lam WL** (2004): Effects of low intensity pulsed ultrasound on fracture healing in aged and young rats. *The 4th Pan Pacific Conference on Rehabilitation. September 24-26, Hong Kong.*
3. **Lam WL**, Guo X, Kwong KSC, Leung KS (2004): Effect of immobilization and neural injury on fracture healing. *The 4th Pan Pacific Conference on Rehabilitation. September 24-26, Hong Kong.*
4. **Lam WL**, Guo X, Kwong KSC, Leung KS (2004): Effect of low intensity pulsed ultrasound on fracture healing. *The 4th Pan Pacific Conference on Rehabilitation, September 24-26, Hong Kong.*
5. **Lam WL**, Guo X, Kwong KSC, Leung KS (2005): Effect of immobilization and neural influence on tibial fracture in rats. *Bone*, 36 (Supp 2): S367.

Effect of peripheral nerve injury on callus formation and fracture healing.

The 23rd Hong Kong Orthopedic Association Annual Congress, November 8-9, Hong Kong.

Hong Kong Journal of Orthopaedic Surgery

11.3

Effect of Peripheral Nerve Injury on Callus Formation and Fracture Healing

Guo X,¹ Lam WL,¹ Kwong SC,¹ Leung KS²

¹Department of Rehabilitation Sciences, The Hong Kong Polytechnic University, Hong Kong; ²Department of Orthopaedics and Traumatology, The Chinese University of Hong Kong, Hong Kong.

Introduction: Mechanical stimulus is being recognized as one of the most important factors influencing fracture healing. It has been shown by recent studies that the skeletal system is innervated with sensory fibers which secrete calcitonin gene related peptide (CGRP) in response to mechanical stimuli. Up to now, there are lack of studies addressing the relationship between bone innervation and fracture healing. The aim of this study is to investigate the role of bone innervation in fracture healing.

Methods: 8 matured female Sprague-Dawley rats (12 weeks of age, around 300 g) have been used for the study. All the rats have received a diaphyseal transverse fracture of the right tibia with an intramedullary pin fixation, then were assigned randomly in equal number into 2 groups: control group, and de-innervation group which received an additional neurectomy of the right sciatic nerve. The rats were sacrificed for tissue analysis at day 21 post fractures.

Results: The average callus index (CI) and fracture union rate (FUR) were 3 and 75% in control group while they were 2.7 and 25% in the group received sciatic nerve resection. There is no significant difference in CI but significant difference in FUR ($p < 0.05$) between control and de-innervation groups.

Conclusion: The results suggest an important role of the sensory nerve innervation in fracture healing. Since injuries of peripheral nerves are common complications associated with fractures, it is essential for us to understand the role of neural influence on fracture healing so as to establish appropriate protocols for treating fractures with neural complications.

Acknowledgement: RGC Grant PolyU 5273/02M.

Effects of low intensity pulsed ultrasound on fracture healing in aged and young rats.

The 4th Pan Pacific Conference on Rehabilitation. September 24-26, Hong Kong.

EFFECTS OF LOW INTENSITY PULSED ULTRASOUND ON FRACTURE HEALING IN AGED AND YOUNG RATS.

Guo, X.¹, Liu, M.Q.^{1,2} and Lam, W.L.¹

¹Department of Rehabilitation Sciences, The Hong Kong Polytechnic University, HKSAR

²Department of Hand Surgery, Beijing Jishuitan Hospital, Peking University, China

Introduction:

Low intensity pulsed ultrasound (LIPU) is an important and effective physiotherapy modality used frequently in enhancing fracture healing. Although numerous animal and clinical studies published since early 80th have confirmed the ability of LIPU to enhance the healing of fractures, the exact physical mechanism has not been established. There are lack of studies addressing the age effect under the LIPU therapy. The aim of this study was to investigate the role of age and LIPU in fracture healing.

Method:

16 matured female SD rats (8 of them 14 months of age, around 800g; the other 8 3 months of age, around 300g) have been used for the study. All the rats have received a diaphyseal transverse fracture of the right tibia with a intramedullary pin fixation, the each age group were randomly divided into two groups (n=4 each group): control group, and daily LIPU treatment group. 3 weeks after operation, bone mineral density (BMD) and bone area (BA) were measured by using quantitative computer tomography (QCT).

Result:

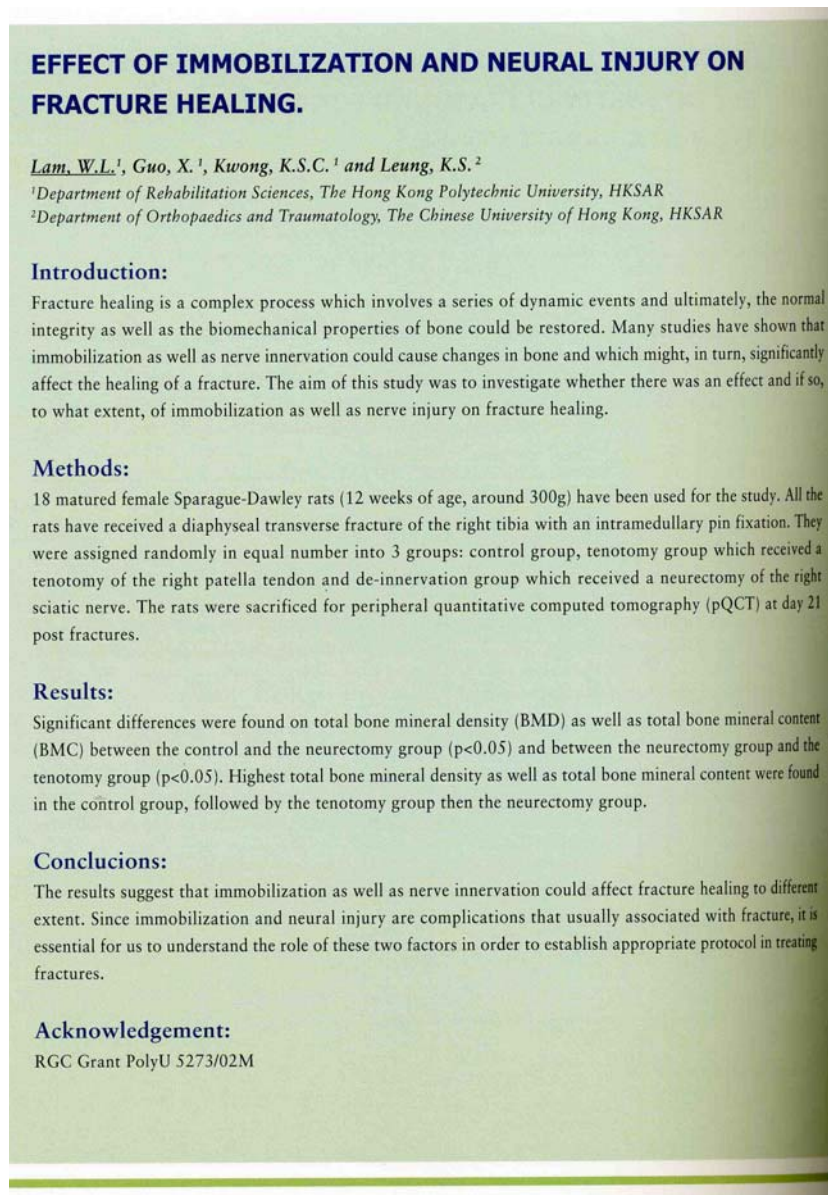
The average callus index (CI) in LIPU group (3.13) was significantly higher than that in control group (2.29). There was no difference between old and young groups. Bone area and callus area (bone are of fracture side minus that of the intact side) of LIPU group were significantly increased than that of the control group ($p < 0.05$). There was no significant difference in bone density between control and LIPU groups.

Conclusion:

The results suggest that low intensity pulsed ultrasound can increase the total bone content and the collagen in bone matrix while the collagen-mineral ratio remains invariable.

Effect of immobilization and neural injury on fracture healing.

The 4th Pan Pacific Conference on Rehabilitation. September 24-26, Hong Kong.



Effect of low intensity pulsed ultrasound on fracture healing.

The 4th Pan Pacific Conference on Rehabilitation, September 24-26, Hong Kong.

EFFECT OF LOW INTENSITY PULSED ULTRASOUND ON FRACTURE HEALING.

Lam, W.L.¹, Guo, X.¹, Kwong, K.S.C.¹ and Leung, K.S.²

¹Department of Rehabilitation Sciences, The Hong Kong Polytechnic University, HKSAR

²Department of Orthopaedics & Traumatology, The Chinese University of Hong Kong, HKSAR

Introduction:

Fracture is a common clinical condition which requires long term rehabilitation. Low intensity pulsed ultrasound (LIPU) is one of the modalities enhancing fracture healing. Promising results were found by using LIPU in accelerating the healing of fractures. The aim of this study was to investigate the accelerating effect of LIPU on fracture healing and mechanisms behind it.

Methods:

12 matured female Sprague-Dawley rats (12 weeks of age, around 300g) were used in this study. A diaphyseal transverse fracture of the right tibia with an intramedullary pin fixation was introduced to all the rats. They were then assigned randomly in equal number into 2 groups: control group and LIPU treated group. Daily LIPU exposure and sham LIPU exposure were given to rats in the LIPU treated group and control group respectively. The rats were sacrificed for peripheral quantitative computed tomography (pQCT) at day 21 post fractures.

Results:

Significant difference was found on the total bone mineral density (BMD) on the fractured tibia between the control and LIPU treated group ($p < 0.05$) with a higher total bone mineral density found in the LIPU treated group.

Conclusions:

The results suggest the promoting effect of LIPU on fracture healing.

Effect of immobilization and neural influence on tibial fracture in rats.

Bone (Volume 36, Supp 2, S367) *The 2nd Joint Meeting of the European Calcified Tissue Society (ECTS) and the International Bone and Mineral Society (IBMS), June 25-29, Geneva, Switzerland.*

ABSTRACTS / *Bone* 36 (2005) S103–S479

S367

Conclusions: Increased LDL-c levels in postmenopausal women were associated with greater probability of lower BMD values and osteopenia. These results suggest that increased LDL-c levels should be regarded as an additional risk factor for lower BMD values in postmenopausal women.

P512-Mo

Growth Retardation and Osteopenia in Adolescents and Young Adults Treated with Hemodialysis

S. O. Mazurenko,¹ M. V. Erman,² R. K. Kuanshkaliev,³ A. A. Enkin⁴

¹Center of Osteoporosis, Medical and Sanitary Unit 122, Sokolov Hospital

²Medical Faculty, Saint Petersburg State University

³Division of Hemodialysis, Saint Magdalene Pediatrics Hospital

⁴Department of Hemodialysis, Leningrad Regional Hospital, Saint Petersburg, Russian Federation

Bone disease and osteoporosis are the major causes of morbidity in end stage renal failure. This study was performed to assess the prevalence and severity of osteopenia and growth retardation in 42 young adults and adolescent dialysis patients, 23 females and 19 males, aged 14–25 years, mean age 19.9 ± 3.85 , with duration of hemodialysis from 1 to 12 years, mean 4.9 ± 3.5 . Bone mineral density of the lumbar spine L1–L4 was measured using dual energy X-ray absorptiometry by Hologic QDR 4500 system. Height and weight were recorded, and body index calculated. Bone age was assessed by analysis of wrist X-rays films. Laboratory investigations included intact parathyroid hormone, serum total and ionized calcium, serum phosphate, osteocalcin, alkaline phosphatase. Mean bone mineral density corrected for gender and age, Z score, of the lumbar spine was -2.01 ± 1.6 . 59.5% had osteopenia or osteoporosis. 45.2% had growth retardation. Growth retardation and a low lumbar bone mineral density were closely associated, $P < 0.001$, with age at start of hemodialysis and pubertal status, duration of hemodialysis and weight, $P < 0.001$. Laboratory results did not correlate significantly with bone mineral density of the lumbar spine. Our results indicated that end stage renal disease and hemodialysis are associated with serious skeletal abnormalities in adolescent and young adults. The start of dialysis before puberty is associated with high risk of growth retardation and developing osteopenia.

P513-Tu

Effect of Immobilization and Neural Influence on Tibial Fracture in Rats

W. Lam,¹ X. Guo,¹ K. S. C. Kwong,¹ K. S. Leung²

¹Rehabilitation Sciences, The Hong Kong Polytechnic University

²Orthopaedics and Traumatology, The Chinese University of Hong Kong, Hong Kong, Hong Kong Special Administrative Region of China

Purpose: To investigate the effect of immobilization and neural influence on fracture healing.

Relevance: Fracture healing is a complex process which involves a series of dynamic events and, ultimately, the normal integrity as well as the biomechanical properties of bone could be restored. Many studies have shown that immobilization as well as nerve innervation could cause changes in bone and which might, in turn, significantly affect the healing of a fracture. Since immobilization and neural injury are complications that are usually associated with fracture, it is essential for us to understand the role of these two factors in order to establish appropriate protocol in treating fractures.

Subjects: Thirty-six matured female Sprague–Dawley rats at 12 weeks of age, around 300 g, have been used in this study.

Methods and materials: All the rats have received a diaphyseal transverse fracture of the right tibia with an intramedullary pin fixation. They were assigned randomly in equal number into 3 groups: control group, tenotomy group, which received a tenotomy of the right patella tendon, and de-innervation group, which received a neurectomy of the right sciatic nerve. The rats were sacrificed for peripheral quantitative computed tomography (pQCT) at day 21 post-fractures.

Analysis: One-way ANOVA was used for all the statistical comparisons between the three groups.

Results: Significant difference was found in both total Bone Mineral Density (BMD) and total Bone Mineral Content (BMC) among three groups ($P < 0.05$). Post hoc analysis (LSD) revealed that control group has a significantly higher total BMD than the neurectomy group ($P = 0.01$). It has also been found that control group has a significant higher total BMC when compared to other two groups (tenotomy, $P < 0.05$; neurectomy, $P < 0.01$).

Conclusions: The results suggest that immobilization as well as nerve innervation could affect fracture healing to different extent.

Acknowledgment: RGC grant PolyU 5273/02M.

P514-Su

Effects of Cyclosporin A on the Remodeling of Alveolar Bone in Rats

C. Wada,¹ H. Seto,¹ T. Nagata¹

¹Department of Periodontology and Endodontology, Institute of Health Biosciences, University of Tokushima Graduate School, Tokushima, Japan

Background: Cyclosporin A (CsA) is used as an immunosuppressant agent. CsA therapy induces side effects such as nephrotoxicity, hepatotoxicity, gingival overgrowth, and osteoporosis. Several studies for CsA-induced osteoporosis have been reported from clinical and basic aspects. Osteoporosis is thought to be one of risk factors of periodontal disease, which is induced by periodontopathic bacteria and resulted in alveolar bone loss. In this study, we